SINK OR SOURCE? RESPONSES OF TUNDRA CARBON FLUXES TO LONG-TERM EXPERIMENTAL WARMING IN A HIGH-ARCTIC POLAR OASIS

by

DECLAN DAWSON TAYLOR

A THESIS SUBMITTED IN PARTIAL FULFILLMENT OF
THE REQUIREMENTS FOR THE DEGREE OF

BACHELOR OF SCIENCE (HONOURS)
(Environmental Sciences)

in

THE FACULTY OF SCIENCE

This thesis conforms to the required standard

_____
Dr. Greg H. R. Henry, Supervisor

THE UNIVERSITY OF BRITISH COLUMBIA
(Vancouver)

MARCH 2022

Table of Contents

Abstract

The Arctic is warming faster than predicted and faster than almost anywhere on the planet. Snowfall, snowmelt, and precipitation patterns are changing, and the active layer is deepening. Soil moisture regimes and growing season length/warmth are changing, affecting the flux of CO_2 into and out of the tundra (net ecosystem exchange; NEE). Tundra regions may shift from sinks to sources of CO_2 emissions with the changing climate.

We examined the effects of ambient and long-term (30+ years) experimental warming on tundra net ecosystem exchange (NEE) of CO_2. NEE is calculated as the sum of the rate of gross ecosystem photosynthesis (GEP) and ecosystem respiration (ER). NEE and ER were measured 3 times over the growing season in and out of passively warmed (1-3ºC) plots (n = 12) using a static chamber system connected to a portable infrared gas analyzer. Plots were established in 1992 and divided evenly across 3 sites representing different soil moisture regimes and plant community types .

Using linear mixed models, we found that warming significantly increased the magnitudes of GEP and ER . Plot greenness significantly explained much of the variation in GEP and NEE. There was a trend of increasing NEE with warming, as the greenness-driven increase in the GEP flux outpaced ER. This evidence suggests that longer and warmer growing seasons may increase NEE and CO_2 sequestration in these plant communities. Comparison with previous results suggest that interannual variability is still greater than variation in multiyear warming trends in the High Arctic tundra.

List of Figures

List of Tables

List of Equations

List of Abbreviations

NEE = Net Ecosystem Exchange

ER = Ecosystem Respiration

GEP = Gross Ecosystem Photosynthesis

GEI = Greenness Excess Index

Introduction

Arctic ecosystems are warming 3-4 times faster than almost anywhere on the planet (Constable et al., 2022; Rantanen et al., 2022). Terrestrial carbon cycles are beginning to change as warming differentially affects ecosystems along environmental gradients (Mekonnen et al., 2021). Impacts include a deepening of the active layer with permafrost degradation, longer growing seasons with decreased snow cover, changes in the surface energy balance, and physiological and phenological plant responses including 'greening' and increased growth (Derksen et al., 2019; Frei & Henry, 2021). Of particular concern is the potential for feedback loops in which warming encourages the transition of terrestrial carbon reservoirs from sinks to sources (McGuire et al., 2009). Tundra ecosystems contain 30-50% of the soil carbon on Earth, an estimated 500 Pg C is in the top metre of permafrost soils (Hugelius et al., 2014; Tarnocai et al., 2009). Warming is accelerating microbial activity and soil organic matter decay in the active layer, generating a permafrost-carbon feedback and hastening the emission of greenhouse gases into the atmosphere (Antala et al., 2022; Koven et al., 2011; Schuur et al., 2015; Skeeter et al., 2022). The High Arctic does not have the same enormous wetland/delta C stocks that are found further south, but is a significant part of the Arctic carbon budget due to its area and potential for greening as vegetation expands across the region (Schuur et al., 2015).

Plants, microbes, and animals mediate the flux between atmospheric CO_2 and terrestrial carbon sequestered into the ecosystem. Net ecosystem exchange (NEE) is the flux of carbon across that boundary, into or out of the ecosystem. NEE is defined as the difference between gross ecosystem productivity (GEP), the total CO_2 drawn into the ecosystem in photosynthesis, and ecosystem respiration (ER), the total respiratory losses of CO_2 from plants and soil to the atmosphere (1).

$$NEE = GEP - ER \quad (1)$$

Ecosystem respiration includes growth, maintenance, and photorespiration by autotrophs, along with heterotrophic respiration from microbes and other soil dwelling detritivores.

The NEE balance determines whether Arctic ecosystems store or release carbon. A positive NEE indicates that GEP exceeds ER, that the tundra is sequestering atmospheric CO_2, whereas a negative NEE indicates GEP is less than ER and a net emission of CO_2. The response of these fluxes to warming will affect a feedback loop either accelerating or decelerating climate change (Davidson & Janssens, 2006). If the respiration response (change in ER flux) is stronger, a positive feedback loop will promote increasing CO_2 emissions with warming as rates of decomposition and heterotrophic respiration rise (Shaver et al., 2000). Conversely, if there is an increase in photosynthesis and growth (the GEP flux increases), a negative feedback loop would slow the emission of CO_2 from Arctic soils.

There is significant heterogeneity in plant community types arrayed across unevenly warming bioclimatic gradients in the Arctic, and ecosystem carbon balance responses to climate change are equally heterogenous (Jónsdóttir et al., 2022; Street et al., 2007). Despite this, closed chamber studies consistently observe that experimental warming increases the magnitude of the photosynthetic (GEP) and respiratory (ER) fluxes (Edwards, 2012; Hobbie & Chapin, 1998; Huemmrich et al., 2010; Jónsdóttir et al., 2022; Lupascu et al., 2014; Oberbauer et al., 2007; Shaver et al., 1998; Welker et al., 2004).

GEP is most significantly driven by variables affecting plants' photosynthetic rates: temperature of the plant canopy, leaf nitrogen content, soil moisture and resource acquisition traits including plant/canopy height, leaf area, and greenness (Arndal et al., 2009; Campioli et al., 2013; Happonen et al., 2022; Jónsdóttir et al., 2022; Street et al.,

2007). Field experiments have demonstrated the link between tundra nutrient availability and increases in GEP, supporting traits like growth, canopy cover, and photosynthetic rates (Betway-May et al., 2022; Mekonnen et al., 2021), and have shown that nitrogen and phosphorus fertilization may increase GEP more than warming (Oberbauer et al., 2007; Shaver et al., 1998).

Over 75% of ER occurs below ground in roots, mycorrhizae, and microbial communities; ER is driven largely by plant and soil microbial activity (Segal, 2013). Canopy temperature (Jónsdóttir et al., 2022) and soil temperature (H.-J. Kwon et al., 2006) are thus key drivers of ER. Soil moisture often determines these warming affects, as soil saturation significantly affects soil oxygen content and thus aerobic decay and belowground respiration rates (M. J. Kwon et al., 2019; Oberbauer et al., 2007). Lowering the water table can turn the tundra from a sink to a source for CO_2 (Huemmrich et al., 2010), despite also encouraging more vigour in plants (Hudson & Henry, 2009).

The factors driving GEP and ER are complex and interactive, and as a result NEE is sensitive to short-term hydrological and climatological shifts (Grant et al., 2011). This is seen in the variable responses to warming and high interannual variability observed in NEE studies, even within the same site (Table S1). Studies often find NEE to be positive (a sink) with variable warming responses between years or sites (Hobbie & Chapin, 1998; Shaver et al., 1998; Welker et al., 2004), or variable in direction and warming response (Oberbauer et al., 2007). Some studies have found a negative feedback loop (positive and increasing NEE; Boelman et al., 2003; Edwards, 2012; Huemmrich et al., 2010), while others have found NEE to be negative and ecosystems become a source of CO_2 with variable to decreasing warming responses (Jónsdóttir et al., 2022).

Eddy covariance studies evaluating NEE on a larger landscape scale have also found that many High Arctic terrestrial ecosystems are currently net sinks for CO_2 (Grant et al., 2011; Lafleur et al., 2012; McFadden et al., 2003), though CO_2 sequestration can occur alongside methane release (Skeeter et al., 2022). Outside the growing season, NEE has a lower, and more negative flux (Arndal et al., 2009; Hobbie & Chapin, 1998; Welker et al., 2004). Wintertime and shoulder-season respiration often result in net CO_2 and CH_4 release (Pirk et al., 2016; Skeeter et al., 2022).

Spectral vegetation indices based on remote sensing techniques are used as proxies for functional traits such as leaf area and canopy photosynthesis (Agger, 2022). The greenness excess index (GEI) can be accurately measured at the plot and individual scale with digital consumer grade cameras (Nijland et al., 2014), and is able to detect differences in vegetation cover and vigour and chlorophyll content (Agger, 2022; Beamish et al., 2016). GEI is well suited to distinguishing plant tissue from soil, an advantage over the normalized difference vegetation index (NDVI), the most common spectral vegetation index in use (Nijland et al., 2014). It has been shown to be an acceptable proxy for SLA, plant cover, and chlorophyll content (Beamish et al., 2016; Edwards & Henry, 2016), and has thus been correlated with increases in GEP (Ahrends et al., 2009; Boelman et al., 2003; Street et al., 2007).

There is an established body of data and literature examining the effects of long term and experimental warming on the tundra carbon balance, and illustrating its continued volatility. Climate change-magnified variations in snowmelt, ecohydrology, and active layer depth can have unpredictable effects on the already significant intra- and interannual variability seen in NEE. In this thesis I investigate the current state and trend of net ecosystem exchange at Alexandra Fiord. I hypothesize that long-term experimental warming

will cause an increasing trend in NEE. GEP and ER are expected to be influenced by GDI and environmental factors such as air and soil temperature and soil moisture, and I explore the relationships between these factors and the fluxes to better understand the controls and drivers of tundra net ecosystem exchange. I spent June through August 2022 on the beautiful coastal lowland at Alexandra Fiord, NU, measuring NEE measurements. The plots have experienced over thirty years of continuous experimental warming and my CO_2 flux measurements were the first on these plots in over a decade and the fifth since 2000. This work contributes to the results from the longest running warming experiment in the circumpolar High Arctic and, through comparison with previous results, furthers our understanding of how NEE and terrestrial ecosystem carbon balances are responding to climate change.

Methods

Study site

Our study was conducted in three sites at Alexandra Fiord (78º53'N, 75º55'W). The sites are arranged on an 8 km^2 deglaciated coastal valley on the eastern shore of Ellesmere Island, Qikiqtaaluk Region, Nunavut, Canada (Figure 1). The three sites in this study sit on Crown land surrounded by Inuit Owned Land under the Nunavut Land Claims Agreement. At approximately 30 m elevation, the study area is nearly flat, sloping northward at 1.5° towards the fiord waters. It is surrounded by steep scree slopes on the east and west sides and the Twin Glacier to the south. Alexandra Fiord is a relatively well-vegetated polar oasis compared to the surrounding polar semi-deserts that characterize much of the High-Arctic (Freedman et al., 1994).

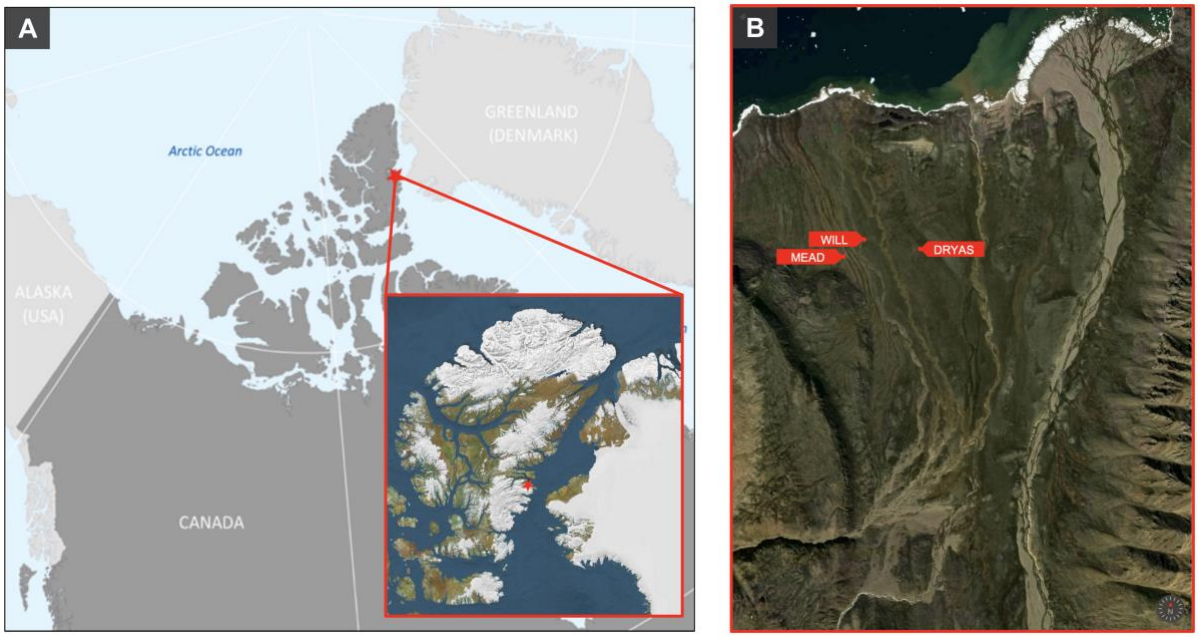

Figure 1. Map of showing the location of (**A**) Alexandra Fiord, NU, in Canada and (**B**) the arrangement of our study sites on the lowland. Satellite image by Maxar Technologies, retrieved via Apple Maps 26 April 2023.

Local variation in ecohydrology, substrate composition, and soil moisture regime create distinct habitats and plant communities across the lowland (Muc et al. 1989). The wet "MEAD" site is a hydric sedge, moss, and dwarf-shrub wetland site dominated by *Eriophorum angustifolium, Carex stans,* and *Carex membranacea*, with flowing surface

water throughout most of the growing season. The moist "DRYAS" site is considered a prostrate dwarf-shrub herb tundra with mesic to hydric soils and less surface water during the growing season. DRYAS is dominated by the woody dwarf shrub *Dryas integrifolia* with prevalent *Cassiope tetragona*, *Arctagrostis latifolia,* and *Carex misandra*. The relatively dry "WILL" site is also a prostrate dwarf-shrub herb tundra but has considerably less snow accumulation, and melted out five days earlier than DRYAS in the 2022 season. WILL is characterized by sandy xeric to mesic soils and is dominated by the deciduous dwarf shrub *Salix arctica*. A relatively large variety of other plants are also present, notably *Luzula confusa, Poa arctica,* and *Papaver radicatum.*

Experimental design

Alexandra Fiord is the founding site of the International Tundra Experiment (ITEX), which is a network of tundra scientists and sites across the polar and alpine tundra biome established in 1990 (Henry et al. 2022). Experimental warming studies were established at Alexandra Fiord in 1992 using open top chambers (OTCs) which heat the enclosed area by 1-3ºC relative to ambient temperature while leaving airflow, RH, and insolation relatively unchanged (Hollister et al., 2022). This warming is within the modeled predictions of Arctic warming and less than the annual temperature variability; OTCs simulate a warm year at a site (Henry et al., 2022). The CO_2 plots had pentagonal OTCs constructed with clear polycarbonate sheets, measuring 0.5 m tall with 1.5 and 2.0 m parallel sides at the top and bottom, respectively (Marion et al., 1997).

Eight plots were established at each of the three sites, with warming chambers installed on half of the plots at each site in 1992: N = 24, n_{site} = 4. The plots were centred on a randomly chosen focal plant species for each site. Plots without OTCs are referred to as control plots and those with OTCs are referred to as warmed (W) plots.

Data Collection

CO2 Flux measurements

We measured growing season net ecosystem CO2 exchange (NEE) and ecosystem respiration (ER) four times in the growing season (July and August, 2022) using an infrared gas analyzer (IRGA; Li-6800, LI-COR Biosciences, Lincoln, NE, USA) connected to a custom-made 75 x 75 x 30cm (168.75L) plexiglass chamber (for details see Welker et al., 2004). Metal collars (75 x 75 cm) were permanently installed in every plot in 1999 to a depth of 15 cm, and the chamber was clamped to the collar forming a closed system with the IRGA. The IRGA measures CO_2 concentration once per second in parts per million (ppm) in air pumped from the chamber, and two fans circulate air in the chamber. Daytime fluxes were measured between 10:30 and 16:30 four times throughout the season, with sites measured on adjacent days. Weather and full-spectrum insolation were comparable on adjacent measurement days we assume that flux measurements were unaffected by changing insolation or relative humidity. Due to logistical complications and mechanical issues, the second measurements of the series are missing at DRYAS and MEAD.

Each flux measurement lasted at least 125 seconds and we omitted the first 5 seconds in which the IRGA would stabilize. Flux measurement periods were kept short, and the chamber air continuously circulated to further reduce the effect of sudden enclosure. NEE was measured during ambient light conditions, followed by the chamber being removed for at least 30 seconds to aerate the plot and chamber, followed by an ER measurement in which the chamber was covered by an opaque polyethylene cloth.

We used linear regression to calculate NEE and ER as the rate of change in CO_2 concentration during the two-minute measurement period. While there is some concern about the suitability of linear regression to model this flux (Kutzbach et al., 2007), visual inspection of our results indicate that it was appropriate for our data, as R^2 values were

found to be up to 0.99 (Figure S1). Results are expressed in µmol CO_2 m^{-2} s^{-1} from the ecosystem perspective where fluxes into the atmosphere are treated as negative and fluxes into the ecosystem as positive (as per Boelman et al., 2003; Edwards, 2012; Oberbauer et al., 2007; Shaver et al., 1998). We calculated GEP as the sum of NEE and RE at each plot (1).

Temperature measurements

Custom made temperature probes for litter (3 cm depth) and air (5 cm height) temperature were fitted to the IRGA chamber. Data output from the Li-Cor 840 and temperature probes were written to proprietary storage modules with a CR-21 datalogger (Campbell Scientific, Inc., Edmonton, AB, Canada).

We measured soil and air temperature using HOBO® Pendant 8K and 64K dataloggers (Onset Computer Corporation, Bourne, MA, USA) positioned immediately adjacent to the chamber bases within the plots for the duration of the field season. Soil Pendants were inserted 5 cm into the soil and air Pendants were mounted 10 cm above the ground under porous white plastic shields to reduce insolation effects. The Pendants recorded temperature every fifteen minutes.

Soil moisture measurements

For each site, we recorded soil moisture in all of the plots each day that CO_2 flux measurements were recorded. In addition, soil moisture was recorded at all plots/sites periodically throughout the season to enrich the moisture record. Readings were taken with a Hydrosense soil moisture probe (Campbell Scientific, Inc., Edmonton, AB, Canada) at three points along the north/south axis of each plot and averaged.

Greenness Excess Index (GEI)

We took digital colour photographs with a Canon EOS Rebel T5 (Canon Inc., Japan), with an 18MP, 5184 x 3465 pixels (px) sensor. The camera settings were consistent throughout the study period (Canon's "intelligent auto" mode). Photos were manually taken from 1.5 m above the ground at nadir.

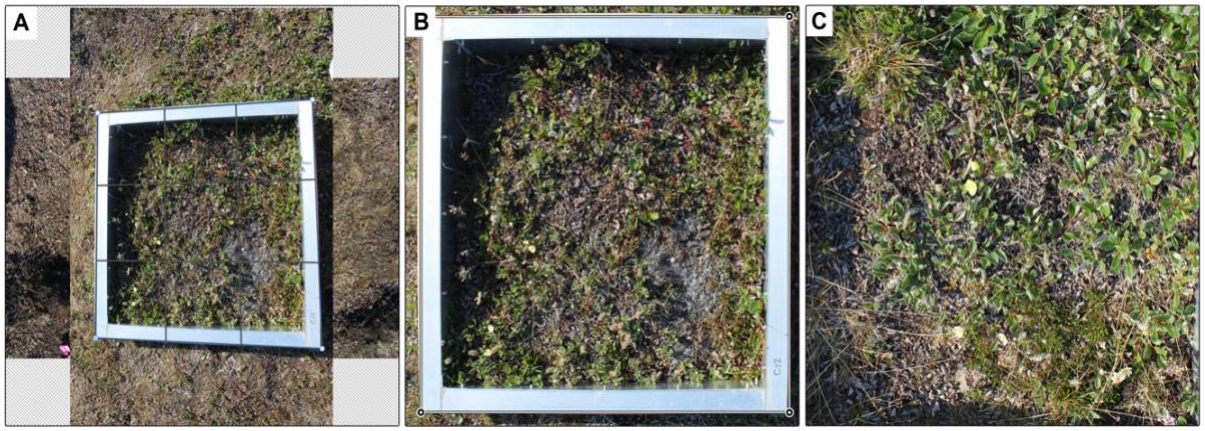

Figure 2. Simplified Adobe Photoshop screengrabs depicting the image processing workflow for plot photos. (A) Images were individually warped to nadir, (B) resized to a common resolution, and (C) cropped to just inside the chamber base.

As per Agger (2022), I processed the images individually in Adobe Photoshop 24.3.0 (Adobe Inc., San Jose, CA, USA, 2022). Photographs for each plot were stacked as layers and each was warped with the *Perspective Warp* feature so that the CO_2 chamber base was perfectly square. This warp corrects for any deviations from nadir (Figure 2A). I then used the *Auto-Align Layers* feature, which automatically aligns images based on shared content, followed by manual adjustments to visually ensure a near-perfect match of the CO_2 chamber base from one layer to the next. I cropped the aligned set to a 1:1 ratio just outside the lip of the chamber base (Figure 2B) before importing it to Adobe Lightroom Classic 12.2.1 (Adobe Inc., San Jose, CA, USA, 2023). I resized all image sets to a common 2000 x 2000px resolution and applied a common 1:1 crop to remove the chamber base (Figure 2C).

The final set consisted of 211 photographs, each one 1750 x 1750 pixels covering an on-the-ground area of approximately 0.5625m^2.

I calculated a greenness value from the standardized images using a function written by Alison Beamish (2011) with the rdgal package in R (v1.6-5, Bivand et al., 2023). Each photograph is imported as a data frame which extracts pixel values from the red (R), green (G), and blue (B) channels. To normalize irradiance variations between images, the green chromatic coordinate, or green ratio (rG) was calculated as:

$$rG = \frac{G}{R + G + B} \quad (2)$$

Red (rR) and blue (rB) ratios were calculated similarly. These ratios are the camera-observed brightness in the reg, green, and blue channels, and are used to calculate the greenness excess index (GEI).

$$\mathrm{GEI} = 2 \times \mathrm{rG} - (\mathrm{rR} + \mathrm{rB}) \quad (3)$$

High GEI indicates a high proportion of green reflectance observed by the camera–which indicates a greater cover of green vegetation in the plot photo (Agger, 2022). Only GEI measurements done on the same day as flux measurements were retained for model analysis described below.

Data loss

A corruption issue prevented data transfer between the data logger and the storage module at the start of the growing season. NEE measurements were acquired by video recording the data logger screen and manually transcribing the video. Temperature measurements were made by manually recording the readout from the chamber temperature probes at the end of the two-minute measurement period. A separate electrical fault resulted in malfunction of the chamber mounted temperature probes; in

these cases, temperature data was substituted with the daytime (10:00-16:00) average from the plot's pendant logger. In one case both the soil temperature probe and pendant logger malfunctioned, so the daytime average of all three other plots of the same (control) treatment was substituted (**Error! Reference source not found.**).

Table 1. Explanation of data collection methods by day and site. Backup methods were employed during various mechanical and electrical errors in the field.

Site	Collection day	CO_2 flux	Temperature
WILL	179	Transcribed video	Chamber probes (start and finish averaged)
	192	Data logger	HOBO logger
	197	Data logger	Chamber probes (continuous)
	208	Data logger	Chamber probes (continuous) except HOBO logger for ER reading in warmed plot 12 T.
MEAD	182	Transcribed video	Chamber probes (start and finish averaged)
	195	Data logger	HOBO logger (control 12 soil averaged from plots 11, 13, 14)
	206	Data logger	Chamber probes (continuous)
DRYAS	183	Transcribed video	Chamber probes (start and finish averaged)
	196	Data logger	Chamber probes (continuous)
	207	Data logger	Chamber probes (continuous)

Data Analysis

Data were assembled in R using the tidyverse collection of packages (Wickham et al., 2019) and the lubridate package (Grolemund & Wickham, 2011) to create a dataframe that included all of the flux data and accompanying environmental parameters. Following the best practices for open science, I designed a coded and reproducible workflow which includes all post-collection work except image processing (Powers & Hampton, 2019; Sandve et al., 2013). A GitHub repository containing raw data; R code for manipulating my data, running analyses, and producing figures; and earlier versions of this manuscript can be found at https://github.com/declan-taylor/honours_thesis. All analyses were done in R version 4.2.2 (R Core Team, 2022).

Carbon fluxes

Three linear mixed models were used for each NEE, ER, and GEP. Models were constructed using lme4 (Bates et al., 2015) and examined for significance using the lmerTest package and Satterthwaite's method for estimating model degrees of freedom (Kuznetsova et al., 2017). The first model included treatment as the single fixed effect and site/plot as random effects with random intercepts and fixed slopes.

$$\text{flux} \sim \text{treatment} + (1|\text{site/plot}) \quad (4)$$

To facilitate a direct comparison between sites and treatments, site was added as a fixed effect for the second iteration of the model to examine differences in plant communities not captured in other variables. Least squares means were compared for each combination of site and treatment factors.

$$\text{flux} \sim \text{treatment} + \text{site} + (1|\text{site: plot}) \quad (5)$$

Finally, a full model was conducted with treatment, site, air temperature, soil temperature, soil moisture, and GEI as fixed effects, and plot as a fixed-slope random effect.

$$\text{flux} \sim \text{treatment} + \text{site} + \text{GEI} + \text{soil moisture} + T_{air} + T_{soil} + (1|\text{site: plot}) \quad (6)$$

Air and soil were highly negatively covariate, so soil temperature was removed. Canopy temperature has been found to be a more significant predictor of carbon fluxes than soil temperature, so it was prioritized (Jónsdóttir et al., 2022). Backwards model selection was done using the step function in lmerTest which eliminates marginal fixed variables and random effect variables to reduce the model's AIC value (Kuznetsova et al., 2017). Model fit was compared via R^2 values extracted using the performance package (Lüdecke et al., 2021).

Environmental parameters

The effect of site and treatment on each of the environmental parameters–greenness, air temperature, soil temperature, and soil moisture–was also examined. A two-way analysis of variance (ANOVA) was constructed for each of the four parameters using the stats package and significance was evaluated with a 95% confidence threshold (R Core Team, 2022).

Results

Carbon Fluxes

Average growing-season daytime NEE was positive at all sites in both treatments (Figure 3). GEP was always positive, and ER was always negative, but gross photosynthesis fluxes were always greater than gross respiration fluxes; the ecosystems consistently acted as a sink for CO_2 (Table 2). NEE across all plots increased in response to warming and was 30.1% higher in the OTC-warmed plots (0.0195 µmol CO_2 s^{-1} m^{-2}) compared with the controls (0.0136 µmol CO_2 s^{-1} m^{-2}). A linear model with treatment as the sole fixed effect did not fit the data well (p = 0.0765, Marginal R^2 = 0.03; Supplementary Table 1). Warming significantly increased the magnitude of both the GEP and ER daytime fluxes, though linear model fit remained poor. The magnitude of ER increased in magnitude by 17.6% from -0.0135 µmol CO_2 s^{-1} m^{-2} to -0.0164 µmol CO_2 s^{-1} m^{-2} (p = 0.00115, Marginal R^2: 0.029;

Supplementary Table 2) and GEP increased 24.5% from 0.0271 µmol CO_2 s^{-1} m^{-2} to 0.0358 µmol CO_2 s^{-1} m^{-2} (p = 0.245, Marginal R^2: 0.035; Supplementary Table 3).

Table 2. Daytime flux values averaged over the growing season. Separated by treatment and by treatment, site. Fluxes are stated in µmol CO2 s-1 m-2. Positive fluxes are those which sequester CO2 into the ecosystem, negative fluxes release CO2 to the atmosphere. See Table 1 for dates of measurements.

Flux	Treatment	Average flux	DRYAS	MEAD	WILL
NEE	ambient	0.01362 ± 0.0140	0.0113 ± 0.0102	0.0074 ± 0.0042	0.0200 ± 0.0184
	warmed (OTC)	0.01948 ± 0.0183	0.0146 ± 0.0098	0.0097 ± 0.0078	0.0305 ± 0.0231
GEP	ambient	0.02708 ± 0.0197	0.0226 ± 0.0117	0.0126 ± 0.0052	0.0410 ± 0.0220
	warmed (OTC)	0.03586 ± 0.0240	0.0294 ± 0.0130	0.0185 ± 0.0095	0.0537 ± 0.0263
ER	ambient	-0.01350 ± 0.0079	-0.0117 ± 0.0034	-0.0052 ± 0.0018	-0.0210 ± 0.0054
	warmed (OTC)	-0.01639 ± 0.0074	-0.0148 ± 0.0049	-0.0088 ± 0.0020	-0.0233 ± 0.0047

All three fluxes varied significantly between sites, with much larger fluxes at WILL compared with DRYAS and MEAD (Figure 3). In the second model, which included site and treatment as fixed effects, NEE varied significantly between DRYAS/WILL (p = 0.0122) and MEAD/WILL (p = 0.0019, Conditional R^2: 0.237, Marginal R^2: 0.226; Supplementary Table 4).

GEP varied significantly between control and warmed (OTC) treatments ($p = 0.0244$), between DRYAS/WILL ($p < 0.001$), and MEAD/WILL sites ($p < 0.001$, Conditional R^2: 0.417, Marginal R^2: 0.414, Supplementary Table 5). ER had the best fit of any of any flux with this model, with means varying significantly between warming and control plots ($p = 0.0012$) and all site combinations (Conditional R^2: 0.758, Marginal R^2: 0.721; Supplementary Table 6). There was no perceivable trend in warming response (relative difference between ambient and OTC-warmed average daytime flux values) across sites and attempts to fit site as a random effect with random slopes and intercepts failed (the model fit was singular). Manual examination of the flux differences between treatment and control plots revealed that that the largest response in NEE to warming occurred at WILL (33.4%), while the largest GEP (32.0%) and ER (41.0%) responses occurred at MEAD (

Table 3).

The final models for NEE, ER, and GEP were different since AIC-based backward selection retained different variables from the full models in (6). NEE was significantly driven by greenness which had a strong positive influence (0.672) on net CO_2 exchange ($p < 0.0001$; Conditional R^2: 0.863, Marginal R^2: 0.822; Supplementary Table 7). Plot ID was retained as a significant random effect in the final model ($p = 0.0119$). ER, by contrast, was affected by a wider suite of parameters. Warming ($p = 0.0348$) and GEI ($p < 0.0001$) both resulted in significantly more respiration, though the GEI effect was far stronger with a parameter estimate that was two orders of magnitude larger (Conditional R^2: 0.846, Marginal R^2: 0.797; Supplementary Table 8). ER also varied slightly but significantly between site ($p < 0.0001$) and plot ($p = 0.0181$). GEP was driven mostly by GEI ($p < 0.0001$), and to a lesser extent by site ($p = 0.0017$; Conditional R^2: 0.848, Marginal R^2: 0.799; Supplementary Table 9). All three fluxes increased in magnitude over the length of the growing season, with the WILL site displaying the largest increases in flux magnitude (

Figure S2).

Figure 3. Boxplots illustrating the effects of experimental warming by OTC (red) against control (blue) temperature regimes on gross ecosystem photosynthesis (GEP), ecosystem respiration (ER), and net ecosystem exchange (NEE). Fluxes responses are significantly different between the mesic DRYAS, hydric MEAD, and xeric WILL sites.

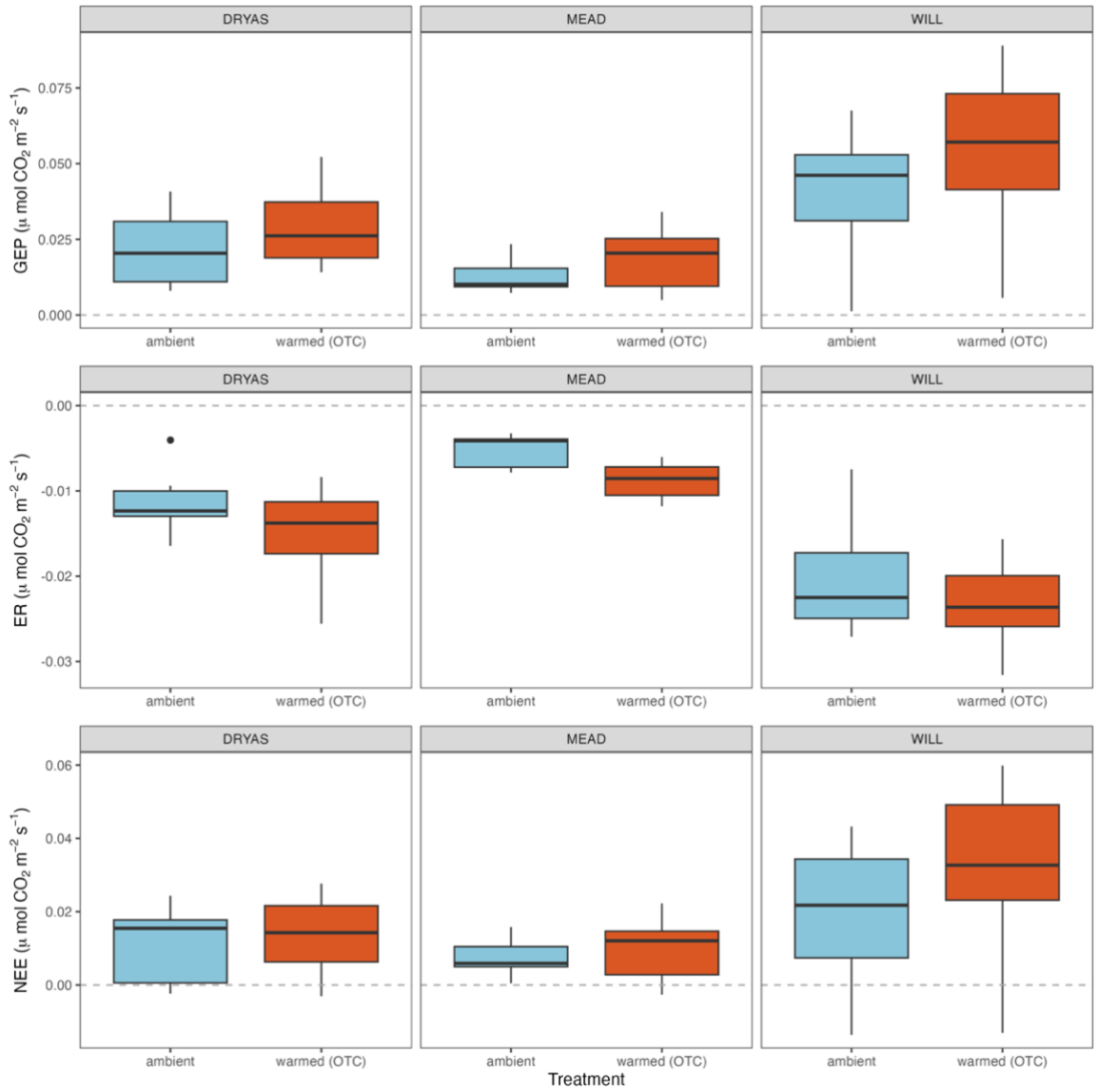

Table 3. Warming response as the difference between ambient and OTC-warmed plot fluxes, for the seasonal daytime average of each flux. Fluxes reported in µmol CO_2 s^{-1} m^{-2} for all sties combined (overall) and by site. The percent difference between the fluxes in the warmed (OTC) and the control plots is also shown.

Flux	Overall	DRYAS	MEAD	WILL
NEE	0.00586 (30.1%)	0.00324 (22.2%)	0.00232 (23.8%)	0.01048 (33.4%)
GEP	0.00878 (24.5%)	0.00676 (23.7%)	0.00592 (32.0%)	0.01273 (23.7%)
ER	-0.00288 (17.6%)	0.00316 (21.3%)	0.00225 (41.0%)	0.00360 (9.67%)

Variable	ANOVA terms	df	Sum of Squares	Mean Squares	F-value	P-value

Soil Moisture	site	2	6.046	3.023	65.655	< 2E-16	***
	treatment	1	0.128	0.128	2.790	0.0991	.
	site*treatment	2	0.218	0.109	2.372	0.1003	
IRGA Air Temperature	site	2	166.2	83.09	7.848	0.00081	***
	treatment	1	6.9	6.88	0.650	0.42287	
	site*treatment	2	3.5	1.77	0.168	0.84598	
HOBO Air Temperature	site	2	564	282.2	21.689	6.18E-10	***
	treatment	1	733	733.8	56.403	1.37E-13	***
	site*treatment	2	142	71.2	5.474	0.00433	**
IRGA Soil Temperature	site	2	166.6	83.29	9.770	0.00017	***
	treatment	1	11.3	11.29	1.324	0.25355	
	site*treatment	2	11.1	5.57	0.653	0.52337	
HOBO Soil Temperature	site	2	1511	755.7	189.76	< 2E-16	***
	treatment	1	17	17.3	4.338	0.0376	*
	site*treatment	2	144	71.8	18.019	2.12E-08	***
GEI	site	2	0.005719	0.002859	7.948	0.00075	***
	treatment	1	0.002719	0.002719	7.558	0.00750	**
	site*treatment	2	0.001429	0.000714	1.986	0.14448	

Table 4. Summary of two-way ANOVAs performed for each of the four environmental parameters: soil moisture, air temperature, soil temperature, and greenness excess index (GEI). Temperature data from the IRGA temperature probe and the HOBO pendant loggers were examined.

Greenness

A two-way ANOVA showed significant variation in GEI across sites ($p < 0.001$) and

treatments ($p = 0.0075$;

Variable	ANOVA terms	df	Sum of Squares	Mean Squares	F-value	P-value	
Soil Moisture	site	2	6.046	3.023	65.655	< 2E-16	***
	treatment	1	0.128	0.128	2.790	0.0991	.
	site*treatment	2	0.218	0.109	2.372	0.1003	
IRGA Air Temperature	site	2	166.2	83.09	7.848	0.00081	***
	treatment	1	6.9	6.88	0.650	0.42287	
	site*treatment	2	3.5	1.77	0.168	0.84598	
HOBO Air Temperature	site	2	564	282.2	21.689	6.18E-10	***
	treatment	1	733	733.8	56.403		***
	site*treatment	2	142	71.2	5.474	1.37E-13	**
						0.00433	
IRGA Soil Temperature	site	2	166.6	83.29	9.770	0.00017	***
	treatment	1	11.3	11.29	1.324	0.25355	
	site*treatment	2	11.1	5.57	0.653	0.52337	
HOBO Soil Temperature	site	2	1511	755.7	189.76	< 2E-16	***
	treatment	1	17	17.3	4.338	0.0376	*

	site*treatment	2	144	71.8	18.019	2.12E-08	***
GEI	site	2	0.005719	0.002859	7.948	0.00075	***
	treatment	1	0.002719	0.002719	7.558	0.00750	**
	site*treatment	2	0.001429	0.000714	1.986	0.14448	

Table 4). Mean GEI increased the most at WILL, slightly at DRYAS, and showed almost no change at MEAD; interaction between plot and site was not significant (p = 0.144). GEI drove a significant amount of variation in all three fluxes, and regressions between GEI and NEE/GEP/ER corroborated the findings of the final linear mixed models. The overall flux-regression slopes did not meaningfully change between warmed and control plots (Figure 4A), though there was some variation when data were separated by site (Figure 4B). WILL had higher flux-GEI correlations than MEAD or DRYAS, which parallel the larger warming effect seen in GEI magnitude at that site. The overall GEP-GEI slopes were steep and positive (control: 0.95, R^2 = 0.751; warmed = 0.92, R^2 = 0.814). ER had weaker relationship with GEI ($R^2_{control}$ = 0.269, R^2_{warmed} = 0.463), with a negative and less

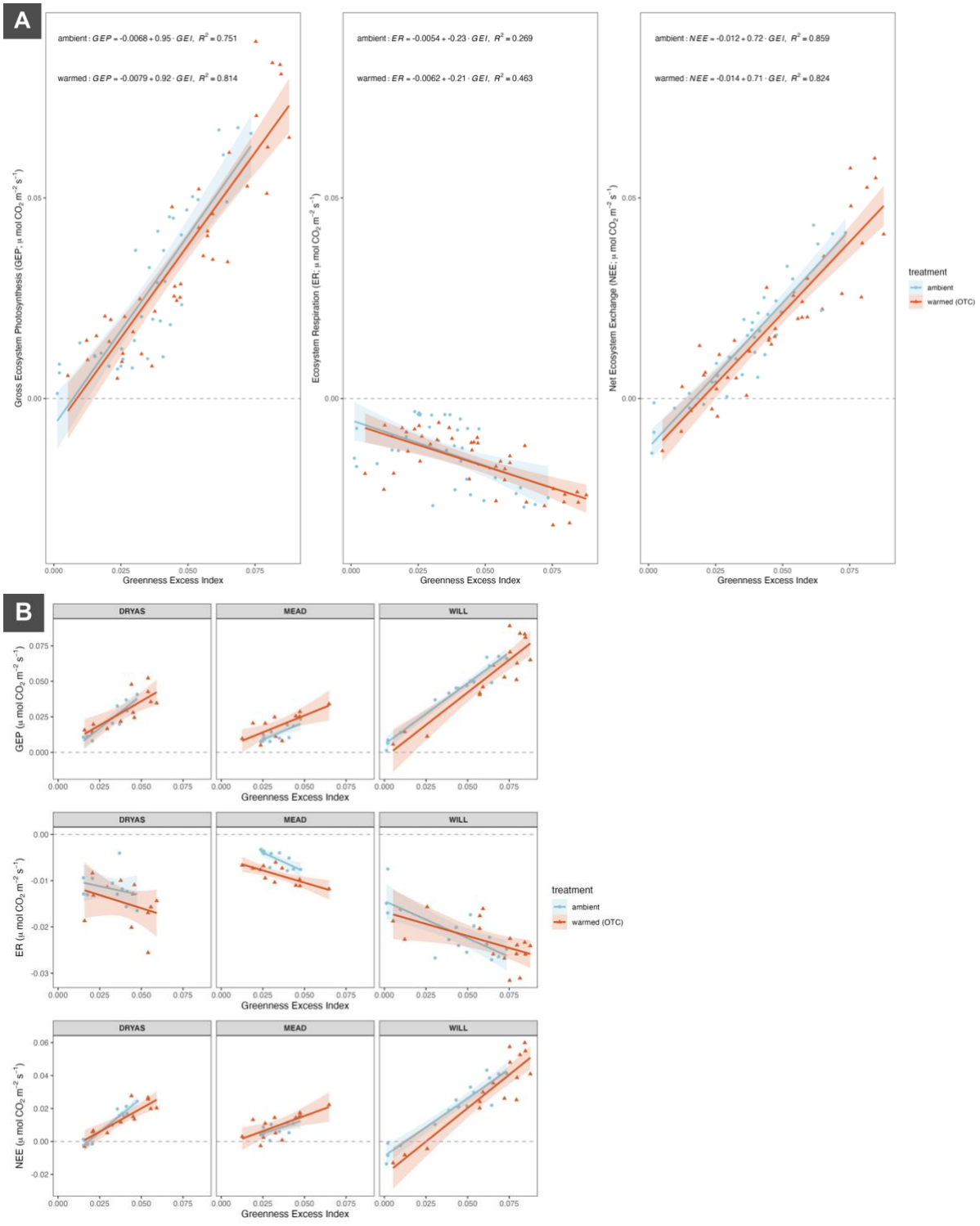

Figure 4. Regressions between GEP and the various ecosystem fluxes. Shown overall (top row) and by site (bottom row), for both treatment and control. Equations and R2 values are given for regression lines not separated by treatment.

steep slope (control = -0.23, warmed = -0.21). NEE and GEI had a very strong relationship, with a tight regression ($R^2_{control}$ = 0.859, $R^2_{ambient}$ = 0.824) and a steep, positive slope (control = 0.72, warmed = 0.71; the difference between the slopes for GEP and ER). The GEI

parameter estimates were similarly positive in the final NEE (0.672; Supplementary Table 7) and GEP models (0.788; Supplementary Table 8), and negative in the final ER model (-0.116; Supplementary Table 9).

Air Temperature

The 10 cm average air temperature measured by the HOBO pendants was 13.5 % higher in the OTC plots (11.1 ºC) than the controls (9.6 ºC;

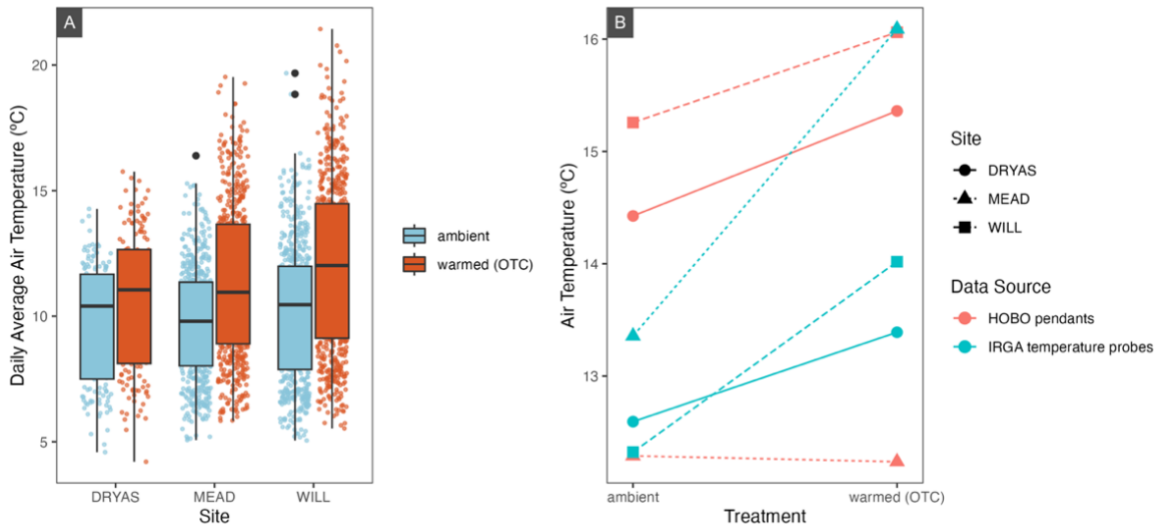

Figure 5A). Daytime air temperatures, or the subset of HOBO readings taken between 1000h and 1600h when insolation was highest and CO_2 flux measurements were performed, were considerably higher: 14.5 ºC in OTC plots and 12.8 ºC in controls. The daytime warming response was smaller than the 24 h difference, 12.1 %, but still significant ($p = 0.0376$). The greatest differences were at MEAD (the overall warmest site) and WILL (Figure 5B). Temperature also varied between sites ($p < 2E\text{-}16$), and the treatment effect was strongly affected by site ($p_{site*treatment} = 2.12E\text{-}08$;

Variable	ANOVA terms	df	Sum of Squares	Mean Squares	F-value	P-value	
Soil Moisture	site	2	6.046	3.023	65.655	< 2E-16	***
	treatment	1	0.128	0.128	2.790	0.0991	.
	site*treatment	2	0.218	0.109	2.372	0.1003	

IRGA Air Temperature	site	2	166.2	83.09	7.848	0.00081	***
	treatment	1	6.9	6.88	0.650	0.42287	
	site*treatment	2	3.5	1.77	0.168	0.84598	
HOBO Air Temperature	site	2	564	282.2	21.689	6.18E-10	***
	treatment	1	733	733.8	56.403		***
	site*treatment	2	142	71.2	5.474	1.37E-13	**
						0.00433	
IRGA Soil Temperature	site	2	166.6	83.29	9.770	0.00017	***
	treatment	1	11.3	11.29	1.324	0.25355	
	site*treatment	2	11.1	5.57	0.653	0.52337	
HOBO Soil Temperature	site	2	1511	755.7	189.76	< 2E-16	***
	treatment	1	17	17.3	4.338	0.0376	*
	site*treatment	2	144	71.8	18.019	2.12E-08	***
GEI	site	2	0.005719	0.002859	7.948	0.00075	***
	treatment	1	0.002719	0.002719	7.558	0.00750	**
	site*treatment	2	0.001429	0.000714	1.986	0.14448	

Table 4). The 5 cm air temperature measurements obtained from the IRGA temperature probes during CO_2 flux measurements varied significantly with site ($p < 0.001$), but not with treatment ($p = 0.423$). MEAD was the coldest and least treatment-responsive site measured by the IRGA probes, opposite to the trend observed by the HOBOs (Figure 5B). DRYAS and WILL were found to be warmer and more responsive.

Soil Temperature

Soil temperature was lower than air temperature throughout the season. Control plots averaged 8.3 ºC in the daytime (1000h to 1600h) and 7.3 ºC over 24h. Treatments (7.9 ºC) were 5.67% colder than ambient plots in the daytime ($p = 0.038$) and 2.68% colder over the 24 h period (7.1 ºC). Figure 6A shows that the responses of soil temperatures to the OTCs were variable between sites; DRYAS decreased, MEAD increased, and WILL showed little response. Daytime mean HOBO soil temperature varied significantly between sites ($p < 0.001$), and mean treatment differences were significantly affected by interaction between site and treatment ($p < 0.001$). Figure 6B illustrates that IRGA measurements captured different site-treatment interactions than the HOBOs. Soil temperatures at DRYAS and

MEAD had opposite responses to OTC presence between measurement tools. Only the effect of site was significant in the IRGA soil temperature measurements ($p < 0.001$; Table 4). Despite the variable OTC response, soil temperatures were much warmer during the day, daytime averages were 12.6% warmer in control plots and 10.0% warmer in OTC plots compared with their 24h equivalents.

Variable	ANOVA terms	df	Sum of Squares	Mean Squares	F-value	P-value	
Soil Moisture	site	2	6.046	3.023	65.655	< 2E-16	***
	treatment	1	0.128	0.128	2.790	0.0991	.
	site*treatment	2	0.218	0.109	2.372	0.1003	
IRGA Air Temperature	site	2	166.2	83.09	7.848	0.00081	***
	treatment	1	6.9	6.88	0.650	0.42287	
	site*treatment	2	3.5	1.77	0.168	0.84598	
HOBO Air Temperature	site	2	564	282.2	21.689	6.18E-10	***
	treatment	1	733	733.8	56.403		***
	site*treatment	2	142	71.2	5.474	1.37E-13	**
						0.00433	
IRGA Soil Temperature	site	2	166.6	83.29	9.770	0.00017	***
	treatment	1	11.3	11.29	1.324	0.25355	
	site*treatment	2	11.1	5.57	0.653	0.52337	
HOBO Soil Temperature	site	2	1511	755.7	189.76	< 2E-16	***
	treatment	1	17	17.3	4.338	0.0376	*
	site*treatment	2	144	71.8	18.019	2.12E-08	***
GEI	site	2	0.005719	0.002859	7.948	0.00075	***
	treatment	1	0.002719	0.002719	7.558	0.00750	**
	site*treatment	2	0.001429	0.000714	1.986	0.14448	

Soil temperature also increased throughout the growing season (Figure S3). At the start of the growing season when we deployed the HOBO pendant loggers, DRYAS and MEAD were quite cold relative to their peak-season temperatures and an increasing trend is visible. Soil temperature at WILL was at its seasonal average at the start of measurements as there is no increasing trend over time (Figure S3).

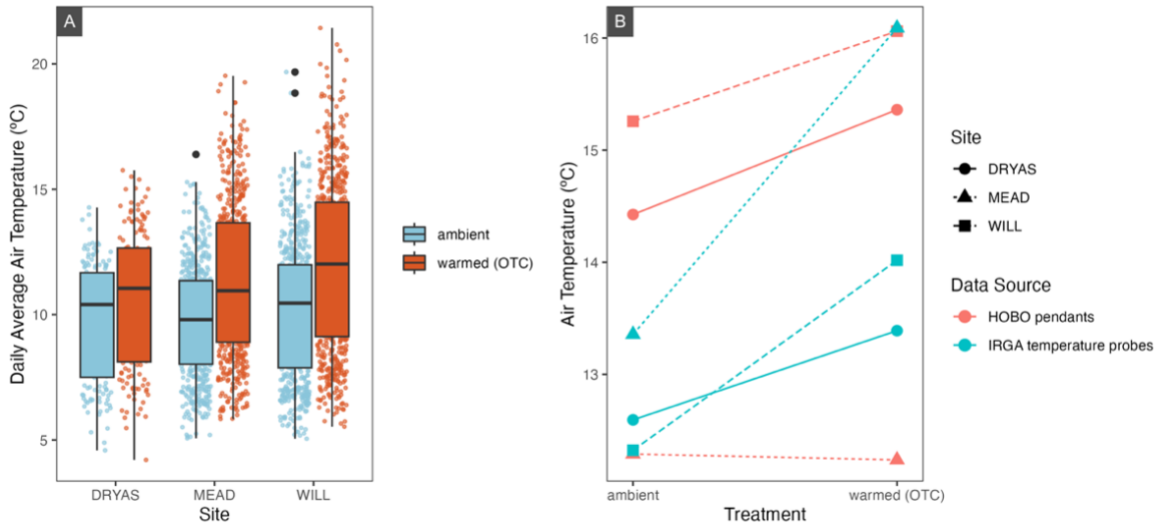

Figure 5. Mean daily air temperature across sites and treatments (**A**). The interaction between site and treatment is illustrated in an ANOVA interaction plot (**B**) for both daytime (1000h-1600h) average 10 cm air temperature, measured every 15 minutes through the growing season by HOBO pendants (orange), and sporadic 20 cm IRGA measurements taken during CO2 flux readings (purple).

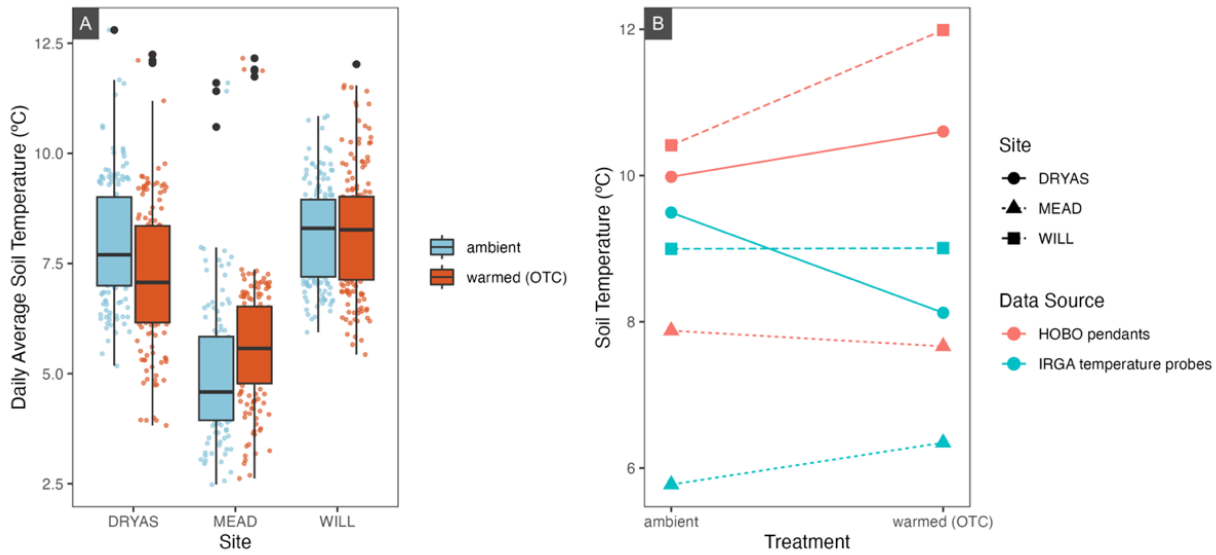

Figure 6. Mean daily soil temperature across sites and treatments (**A**). The interaction between site and treatment is illustrated in an ANOVA interaction plot (**B**) for both daytime (1000h-1600h) average soil temperature, measured every 15 minutes through the growing season by HOBO pendants (orange) embedded 5cm in the soil, and sporadic IRGA measurements taken during CO2 flux readings (purple), embedded 3cm into the litter.

Soil Moisture

Soil moisture averaged over the growing season was 63% at MEAD, the highest of any site, 33% at DRYAS, and 36% at WILL. The variance between sites was significant ($p < 2E-16$), and the variance between treatments was not significant ($p = 0.099$;

Table 4). Control plots in MEAD were much wetter than OTC plots, where in WILL and DRYAS they were dryer, though interaction between site and treatment was not significant (p = 0.100).

Variable	ANOVA terms	df	Sum of Squares	Mean Squares	F-value	P-value	
Soil Moisture	site	2	6.046	3.023	65.655	< 2E-16	***
	treatment	1	0.128	0.128	2.790	0.0991	.
	site*treatment	2	0.218	0.109	2.372	0.1003	
IRGA Air Temperature	site	2	166.2	83.09	7.848	0.00081	***
	treatment	1	6.9	6.88	0.650	0.42287	
	site*treatment	2	3.5	1.77	0.168	0.84598	
HOBO Air Temperature	site	2	564	282.2	21.689	6.18E-10	***
	treatment	1	733	733.8	56.403		***
	site*treatment	2	142	71.2	5.474	1.37E-13	**
						0.00433	
IRGA Soil Temperature	site	2	166.6	83.29	9.770	0.00017	***
	treatment	1	11.3	11.29	1.324	0.25355	
	site*treatment	2	11.1	5.57	0.653	0.52337	
HOBO Soil Temperature	site	2	1511	755.7	189.76	< 2E-16	***
	treatment	1	17	17.3	4.338	0.0376	*
	site*treatment	2	144	71.8	18.019	2.12E-08	***
GEI	site	2	0.005719	0.002859	7.948	0.00075	***
	treatment	1	0.002719	0.002719	7.558	0.00750	**
	site*treatment	2	0.001429	0.000714	1.986	0.14448	

Discussion

We examined the net ecosystem exchange of CO_2 (NEE) and its component fluxes across temporal and environmental gradients to capture change in carbon fluxes throughout the growing season, across soil moisture gradients, and between plant communities. NEE is the balance of GEP and ER, two climactically controlled processes that vary with plant traits, ecosystem drivers, and scale. Across the Arctic, variability in the magnitude of GEP and ER warming responses results in tundra systems being sinks, or sources of CO_2, depending on site conditions (Virkkala et al., 2018). There is a dearth of long-term data and measurements from more extreme High Arctic environments, especially in the Canadian archipelago, making our repeat high-Arctic experiment of particular value (Virkkala et al., 2018).

Fluxes, greenness, and carbon sequestration

Net ecosystem exchange was positive across all treatments and sites. The average carbon balance at Alexandra Fiord (during day-time hours in the growing season) was positive, and thus the ecosystem was acting as a sink. Experimental warming by OTCs increased the magnitudes of both the GEP and ER component fluxes, and since the increase in GEP was larger, NEE increased by 30%. These results indicate that warming promotes further carbon sequestration. As NEE is not itself a process but the balance between two processes–photosynthesis (GEP) and respiration (ER)–the often-overlapping drivers of these two fluxes and the interactions between them collectively determine the magnitude and direction of the ecosystem carbon balance.

Gross ecosystem productivity

Marchand et al. (2004) outline that GEP in warmed plots may be elevated due to the acceleration of the temperature-linked biochemical processes (enzyme kinetics) in

photosynthesis, or indirect effects, such as warming-driven changes in nutrient uptake, leaf area, or species composition. Tundra plants generally have with low temperature optima for photosynthesis (Tieszen, 1973) and acclimatize to new temperature regimes (Billings et al., 1971; Marchand et al., 2004). Some recent closed chamber studies have found that canopy temperature, measured as a microclimatic (plot level) parameter, played a dominant role in driving variation in GEP fluxes after long-term warming (Jónsdóttir et al., 2022), but our models did not retain these parameters, and we did not observe significant differences in them between plots of different treatment manipulations. Given that our OTCs have been warming the treatment plots for over three decades, it seems unlikely that direct effects are the dominant reason for the increases in GEP.

There is a well-documented link between warming and the acceleration of plant growth (Bjorkman et al., 2018; Campioli et al., 2013; Frei & Henry, 2021; Hudson et al., 2011). Greenness, or GEI, captures an index of the amount of active plant leaves in a plot by proxying plant size, leaf area, and photosynthetic capacity (Beamish et al., 2016; Boelman et al., 2003; Nijland et al., 2014). Our warmed plots were greener, and GEI had a strong relationship with GEP and explained the most variation in GEP. These results indicate that increased indirect effects that result in greater greenness are the likely drivers of increased GEP, and higher net carbon sequestration.

GEP varied significantly between sites, and site was retained as the only other significant fixed effect in our final GEP model. The meadow site (MEAD) is dominated by graminoids and, due to the absence of large grazers on the landscape at Alexandra Fiord, has considerable amounts of litter (Henry et a 1986; Hill and Henry 2011). DRYAS is somewhat of an intermediate site in terms of species composition, soil moisture, and litter

volumes. WILL is dominated by a deciduous shrub, *Salix arctica,* and is relatively free of litter. The relationship between GEI and GEP as strongest at WILL.

In addition to questions of litter and greenness, site also captures variation in plant community. Interspecific variation in plant traits and phenology likely explain variation in GEP. The WILL site is warm with less snowfall, earlier snowmelt, and dryer soils. In addition, *Salix arctica* is one of the earliest species to flower and green up (Bjorkman et al., 2015). For both of these reasons the plants at WILL likely had earlier phenology than plants at DRYAS and MEAD. Coupled with their high photosynthetic capacity (Oberbauer et al., 2007), this temporal and compositional difference likely drove larger photosynthesis fluxes. High GEP fluxes have been associated with woody shrub presence elsewhere (Cahoon et al., 2012), though a recent review paper suggests that graminoid sites have the highest peak season GEP (Virkkala et al., 2018). However, the authors largely attribute this to leaf area and metabolic speed and leaf area is limited at our graminoid site (MEAD) as senesced leaves make up far more of the canopy coverage than active live leaves. Inter site differences at Alexandra Fiord also may have been magnified by low soil moisture at WILL; *S. arctica* is more vigorous at well-drained sites than elsewhere on the lowland (Beamish et al., 2016). The DRYAS site, also rich in prostrate dwarf shrubs, melts out later and is has been victim to flooding which has raised the water table and promoted a shift towards graminoids over the last decade (G. Henry, *pers. comm.*, 2022).

Light intensity and incident photosynthetically active radiation (PAR) play a dominant role in photosynthesis rates (Tieszen, 1973) and have been strongly linked to NEE rates in the field (Skeeter et al., 2020). Like many plants in open environments, Arctic plants are shade intolerant and vary sensitive to changes in light levels. Plants are rarely light-saturated, and GEP is highly sensitive to PAR (Edwards, 2012; Tieszen, 1973). Leaf nitrogen

commonly also limits or drives photosynthesis rates (Arndal et al., 2009; Evans, 1989). This has been corroborated by field (Betway-May et al., 2022; Jónsdóttir et al., 2022) and fertilization experiments (Boelman et al., 2003; Shaver et al., 1998). We did not measure incident PAR or the size of the nitrogen pool, but some of the unexplained variation in our models is likely due to these two parameters. Overall, we can conclude that while we have not captured the full diversity of factors affecting GEP, plant community, canopy cover, leaf area, and photosynthetic capacity play significant roles in determining this flux and the overall carbon balance.

Ecosystem respiration

Ecosystem respiration is the cumulative respiratory efflux of carbon dioxide from plants (photorespiration, growth, and metabolic processes), mycorrhizal networks, soil microbes, and other detritivores. The belowground component of ER comprises most of the ecosystem's total CO_2 release (Liu et al., 2022; Marchand et al., 2004). Variation in our ER measurements was explained by site, treatment, and GEI. GEI was the largest and most significant influence, likely because it is an index of biomass and plant/canopy size. More above-ground plant tissue is associated with higher ER fluxes because larger plants have larger root and mycorrhizal networks and higher litter production. These traits are associated with higher soil microbial activity and soil organic matter decomposition [cite; potentially Bjorkman et al 2020]. Ecosystem respiration fluxes were largest at WILL which has large carbon stocks and steady litter production from deciduous woody shrubs. Unlike MEAD however, high litter production at WILL is likely matched by greater decomposition rates and litter does not accumulate. Compared with GEP and NEE, the GEI-ER regression trendline was relatively shallow and poorly fit both overall and at each site, suggesting that this flux is significantly driven by other factors.

Site and treatment variation may support an ER-climate change positive feedback loop mechanism described by Grant et al. (2011). They suggest that warming promotes permafrost thaw, which generates a deeper, warmer active layer for longer in the summer, which enables increased decomposer activity, carbon remineralization, and CO_2 efflux. ER fluxes are higher at the OTC-warmed sites, aligned with strong experimental evidence supporting the strong dependency of ER on temperature (Cahoon et al., 2012; Jónsdóttir et al., 2022), as temperature limitations on enzyme kinetics, as well as active layer freezing, can dramatically slow carbon mineralization (REF).

Model results and excluded parameters

NEE was 30% higher in warmed plots and GEP, ER varied significantly between sites; treatment was a small but significant predictor of variation in the ER final model. Backwards selection removed air temperature, soil temperature, and soil moisture from our GEP, ER, and NEE full models. This status, and the associated small parameter estimates of these environmental parameters, suggests that they do not explain a significant amount of variation in any of our observed fluxes. This is in contrast to much of the literature on ecosystem carbon balances, which often find trends between each flux and in situ air/soil temperature and soil moisture.

Temperature and OTC-warming responses

Air and soil temperature were removed from the final flux models, though our results demonstrate that the temperature measurements captured by the IRGA probes during CO_2 flux measurements are likely a poor approximation of the seasonal temperature record. This makes sense because while the HOBO pendants measured the surrounding air/soil temperature in and out of the OTCs, the IRGA temperature probes consistently measured temperature while the OTCs were temporarily off the plots, but the IRGA

chamber was sealed. We thus would not expect the IRGA probes to model OTC differences. Given that CO_2 fluxes are dependent on a variety of plant traits and ecosystem drivers that are themselves dependent on long-term climatological conditions, OTC presence likely captures a suite of warming-based effects that drive variation between treatments.

Soil temperature responded unevenly to OTC presence, but air temperature was consistently warmer. This is in line with recent ITEX-wide findings which suggest a decoupled air/soil temperature OTC response (Hollister et al., 2022). Given that experimental and long term warming have increased vegetation cover in many experimental plots, soil temperatures may not match air warming trends due to increased shading (Elmendorf et al., 2012a, 2012b), Recent ITEX analyses also suggest that there is little species composition change in and out of the OTCs (Henry et al., 2022), affirming the robustness of OTCs as a method of experimental manipulation that can guide our understanding of vegetative climate-warming responses (Hollister et al., 2022).

Soil moisture

Soil moisture varied significantly between sites and had opposite warming responses in different sites. Water content was lower in warmed plots at DRYAS and WILL but higher at MEAD, and didn't follow a clear seasonal trend at any of the sites. Rather than indicating a strong treatment-site interaction, these results are likely due to soil moisture varying based on local hydrological conditions unique to each site.

It is common to see interactions where soil moisture affects the warming response of plant traits (Bjorkman et al., 2018) and the magnitude and direction of ecosystem carbon fluxes (Oberbauer et al., 2007; Shaver et al., 1998). Huemmrich et al. (2010) and Oberbauer et al. (2007) both provided strong evidence for temperature-soil water content interactions, experimental manipulations of temperature and soil moisture found positive correlations

between each of these and NEE, with synergistic effects between the factors. Especially in hydric ecosystems, soil water content can be high enough that anoxic conditions in soils limit belowground respiration (Oberbauer et al., 2007), and on an ecosystem scale, a high water table can reduce the mineralization and efflux of CO_2 (Knoblauch et al., 2013; M. J. Kwon et al., 2019). The anoxia-ER relationship is also well documented in Low Arctic studies examining permafrost-carbon feedbacks (Knoblauch et al., 2013; H.-J. Kwon et al., 2006; M. J. Kwon et al., 2019).

It was unexpected that our data did not present a relationship between soil moisture and ER, especially given the significant variation between the hydric and often-saturated soil conditions at MEAD, and the well-drained xeric conditions at WILL. The MEAD site had the highest soil moisture and the lowest ER, although it was not significantly different from the other two sites. One potential explanation is that large quantities of root and rhizome biomass likely account for the bulk of belowground ER at MEAD (G. Henry, *pers. comm.*, April 2023), where microbial ER is more prominent in the other sites. Even if microbial respiration rates were dramatically reduced at MEAD, we might still capture a weak gradient with soil moisture because root, rhizome, and mycorrhizal respiration collectively offset this difference. Huemmrich et al. (2010) suggest that the corollary to anoxic flux limitations is that soil saturation should also limit ER responses to temperature. Our data is opposite to this–at MEAD, ER has the strongest increase in magnitude with warming. Where the warming response of soil microbes and detritivores is almost completely dependent on soil temperatures, which are reduced through shading and somewhat decoupled from the OTCs, belowground plant tissues can also respond to aboveground warming. ER might increase through receiving additional photosynthates and other benefits from the rest of the plant experiencing higher air temperatures.

Long term trends

Our 2022 measurements at Alexandra Fiord were the fifth since 2000, contributing another landscape-level observation to our long-term warming experiment. I examined nine other similar chamber-based studies, which represent ongoing work at Alexandra Fiord (Nunavut), Toolik Lake (Alaska), and Utqiagvik (Alaska), along with more intermittent work at other sites across the circumpolar High Arctic (Table 5). Our results are similar to other warming manipulations on High Arctic carbon balance: GEP and ER nearly always increase in magnitude in response to warming, with variable responses in NEE. Mean daytime growing season NEE increased more often than it decreased, which is supported by landscape-scale eddy covariance work in the Low Arctic (Grant et al., 2011; McFadden et al., 2003; Skeeter et al., 2022). A review study of global Arctic and sub-Arctic chamber studies also found that NEE had variable warming responses (Virkkala et al., 2018). The complex of interacting environmental variables which determines fluxes and carbon balance are sensitive enough that intra-annual and inter-site variability appear to be larger than long-term warming responses, making it difficult to draw conclusions about climate-NEE feedback loops.

Comparing our results with previous results from Alexandra Fiord, we see a positive trend in NEE at DRYAS. The negative NEE values seen in 2000 and 2001 at DRYAS were negligible in 2011 and positive in 2022. The variable warming responses of the fluxes have also become more positive. While we could speculatively associate the trend of increasingly positive NEE and warming responses with long-term warming from climate change and 30+ years of OTC presence, it is also certainly driven in part by hydrological changes on the

Table 5. Flux responses from published field studies at sites across the High Arctic.

Source	Place	Tundra characteristics	Year(s)	NEE	NEE response	GEP response	ER response
(Hobbie & Chapin, 1998)	Toolik Lake (inlet and outlet), AK	Wet sedge tundra	1993	Sink	↕ (across sites)	↑	↑
(Shaver et al., 1998)	Toolik Lake (inlet and outlet), AK	Wet sedge tundra	1994	Sink	↕ (across sites)	↑	↑
(Boelman et al., 2003)	Toolik Lake outlet, AK	Wet sedge tundra	2002	Sink	↑	↑	–
(Marchand et al., 2004)	Zackenberg, NW Greenland	Mesic mosaic tundra	1999	Sink	↑	↑	↑
(Welker et al., 2004)	Alexandra Fiord	Wet sedge meadow	2000- 2001	Sink	↓	↓	↑
		Mesic meadow		Source	↑	↑	↑
		Xeric heath		Sink	↑	↑	↑
(Edwards, 2012)	Alexandra Fiord	Wet sedge meadow	2011	Sink	↑	↑	↑
		Mesic meadow		Sink	↓ (slight	–	–
		Xeric heath		Sink	↑	↑	↑
(Oberbauer et al., 2007)	Toolik Lake, AK	Mesic tussock	1997-1998	Source	↓	↓	↓
		Xeric heath		Source	↓	↑	↑
	Alexandra Fiord, NU	Wet sedge meadow	2000-2001	Sink	↕ (across years)	↓	↑
		Mesic meadow	(Alex,	Source	↑	↑	↑
		Xeric heath	Utqiagvik,	Sink	↕ (years)	↑	↕
	Utqiagvik, AK	Wet tundra	Atqasuk)	Sink	↑	↑	↑
		Dry tundra		Source	↓	↑	↑
	Atqasuk, AK	Wet tundra		Sink	↑	↕	↓
		Dry tundra		Source	↓	↑	↑
(Jónsdóttir et al., 2022)	Endalen Valley, Svalbard	Deep snowbed, *Cassiope* heath, *Dryas* heath (least snow).	2018	Source or negligible	↑ *in magnitude*, (↓ when NEE a source)	↑	↑
(Huemmrich et al., 2010)	Utqiagvik, AK	Wet sedge tundra	1999-2001	Sink	↑	↑	↑

landscape. DRYAS in particular has had significant enough changes in moisture regime that it would be impossible to isolate a single driver of long-term change.

Of particular interest in the long term may be the impacts of shrubification, the process by which deciduous shrubs with taller maximum canopy heights advance. As patches are infilled and prostrate shrubs increase growth, these plants may come to dominate tundra ecosystems as they warm (Mekonnen et al., 2018, 2021). Shrubification can affect flux rates by favouring larger plants and species with higher photosynthesis rates and increasing litter production and thus soil respiration (Finderup Nielsen et al., 2019; Virkkala et al., 2018). Our deciduous dwarf shrub-dominated site had the largest carbon fluxes, and compositional shifts towards woody shrubs have been noticed at the MEAD and DRYAS sites (i.e. those not already dominated by *S. arctica*; Edwards & Henry, 2016). Changing species composition and hydrological conditions will certainly continue to affect NEE into the future.

Year-round fluxes

While we have seen increases in GEP, ER, and NEE during the summer, we did not measure shoulder season fluxes at Alexandra Fiord. Across the Arctic, photon flux density has been shown to play a significant role in photosynthesis rates and carbon flux magnitudes, and drives diurnal and seasonal patterns in GEP and NEE (Skeeter et al., 2020). GEP ramps up through the spring with leaf bud expansion, and declines throughout the fall with decreasing daylight hours and photon flux density (Uchida et al., 2016); carbon assimilation stops completely while the active layer is completely frozen and plants are covered with snow (Pirk et al., 2016). When incident light is low but shoulder season temperatures are mild (especially typical of the early to mid-autumn), respiration does not decline with photosynthesis and instead drives a negative NEE flux (Christiansen et al.,

2012), also experimentally observed at Alexandra Fiord (Welker et al., 2004). Respiration continues throughout the year, but flux magnitudes are much smaller in the winter, with observable effluxes of both CO_2 and methane (Christiansen et al., 2012; Pirk et al., 2016).

This trend prevents us from extrapolating conclusions about whether our site is a net sink of carbon sequestration beyond daytime hours in the growing season. To understand the complete impact of the tundra on atmospheric CO2 concentrations, one would need to do 24-h/day measurements throughout all seasons; a logistical impossibility for researchers who do not live at their field site and are constrained to diurnal field practices. While winter and nighttime GEP fluxes are lower than the growing season daytime, Welker et al. (2004) found that the flux magnitudes at those times were small enough that they did not dominate the carbon balance and did not change NEE from a sink to a source at our site. Growing season daytime fluxes are the largest of any time of day or year, and so remain the most important drivers of net year-round ecosystem carbon balance.

Conclusion

We measured carbon dioxide fluxes at three sites in the Alexandra Fiord valley on Ellesmere Island, NU. Our sites represented a diversity of plant communities with species compositions varying along a soil moisture gradient. Our results conclusively showed that this High Arctic tundra is acting as a net sink of carbon throughout the day during the growing season. Warming manipulations demonstrated that experimental warming, a simulation for climate change, drives larger fluxes and increases the sequestration of CO_2 in all three plant communities. The xeric dwarf shrub site dominated by *Salix arctica* demonstrated the largest fluxes and response to warming. Greenness excess index, a proxy for biomass, leaf canopy, and photosynthetic capacity, was by far the most important driver of NEE and its component fluxes, ER and GEP. The stronger relationships between GEI and GEP/NEE compared with ER indicates that plant size as measured by greenness has more influence on carbon assimilation, and efflux is likely determined by other factors including more direct links with temperature and soil moisture and belowground processes. NEE studies should continue into the future to observe how ecohydrology and species composition continue to affect Arctic carbon fluxes.

Acknowledgements

I had the privilege of spending the summer on Ellesmere with Sofie Agger, Brittney Miller, Nicola Rammell, and my supervisor, Greg Henry. I am gratefully indebted to their warmth, senses of humour, musical talents, cooking abilities, and work ethics: they made my time at Alexandra Fiord incredibly educational and fun. Brittney, Nicola and Greg assisted in data collection for the flux measurements. Courtney Collins and Cassandra Elphinstone provided guidance on the modelling and analysis of my data. Dr. Greg Henry was both the architect of the Alexandra Fiord warming experiment and this particular project–I thank him particularly for his support, encouragement, coaching, and mentoring as I analyzed our data and prepared this manuscript.

As scientists we had the privilege of living and working out of six buildings on the lowland constructed by the RCMP in the early 1950s as part of a forced relocation of Inuit from Nunavik and Baffin Island by the Canadian government to assert their colonial sovereignty over the High Arctic Archipelago. Our research site sites on Crown land, and land owned by the Qikiqtani Inuit Association under the Nunavut Land Claims agreement. I am grateful for the opportunity to have been able to visit and work at Alexandra Fiord and learn about the North.

Our work was funded by the Canada Foundation for Innovation, Polar Knowledge Canada, and the Natural Sciences Engineering and Research Council. The field research was conducted under a Wildlife Research Permit from the Nunavut Department of Environment (number).

Author's Note

This manuscript is the product of burnt midnight oil (metaphorical carbon), burnt jet fuel (real carbon), and a lot of chocolate covered almonds. Even so, it feels like it's missing something. I would be remiss if I didn't remark on how this project change me. I am ocean person at heart, and had always focused my academic lens on the rocky, briny shores of the British Columbia coast. That is, until May 2022, when I boarded a plane and headed North. Alexandra Fiord is a truly magical and transformative place, it offers a rare opportunity to live beyond the reach of roads, phones, internet, plumbing, and even darkness.

This manuscript is missing involuntary, helpless grin I couldn't wipe off my face at the taste of fresh blueberry scones, and the pure joy that eating brought all summer.

This manuscript doesn't tell the story of the night on which Nicola and I danced around the main building at Alex Fiord to Joni Mitchell, the eleven p.m. sun reflecting off the sea ice through the kitchen windows, crying, not because anything was wrong, but because of how beautiful and simply *astonishing* it was to listen to Joni Mitchell three hundred kilometers from anyone else on the planet.

This manuscript is silent. You can't hear the crackle of our VHF radio as High Arctic field camps called in their 'good mornings' to the base in Resolute, or Greg softly strumming our taped-up, polar bear-cracked guitar, and teaching me to do the same. You can't hear your ears ring in silence that characterized the fiord on windless spring mornings before the streams started to flow.

Perhaps a thesis isn't supposed to capture all of those things, but they remain an integral part of the experience of conducting this research for me. And I'm generally not a believer in separating researcher from research, so I wanted to share. Thank you for reading–I'm proud of this thesis, and hope it wasn't too much of a slog to mark.

Works Cited

Agger, S. (2022). *Greening responses to long-term experimental warming in high arctic tundra communities using plot-level remote sensing* [M.S. thesis]. The University of British Columbia.

Ahrends, H. E., Etzold, S., Kutsch, W. L., Stoeckli, R., Bruegger, R., Jeanneret, F., Wanner, H., Buchmann, N., & Eugster, W. (2009). Tree phenology and carbon dioxide fluxes: Use of digital photography for process-based interpretation at the ecosystem scale. *Climate Research*, *39*(3), 261–274.

Antala, M., Juszczak, R., van der Tol, C., & Rastogi, A. (2022). Impact of climate change-induced alterations in peatland vegetation phenology and composition on carbon balance. *Science of the Total Environment*, *827*, 154294. https://doi.org/10.1016/j.scitotenv.2022.154294

Arndal, M. F., Illeris, L., Michelsen, A., Albert, K., Tamstorf, M., & Hansen, B. U. (2009). Seasonal Variation in Gross Ecosystem Production, Plant Biomass, and Carbon and Nitrogen Pools in Five High Arctic Vegetation Types. *Arctic, Antarctic, and Alpine Research*, *41*(2), 164–173. https://doi.org/10.1657/1938-4246-41.2.164

Bates, D., Mächler, M., Bolker, B., & Walker, S. (2015). Fitting Linear Mixed-Effects Models Using lme4. *Journal of Statistical Software*, *67*(1), 1–48. https://doi.org/10.18637/jss.v067.i01

Beamish, A. L. (2011). *The use of repeat colour digital photography to monitor high Arctic tundra vegetation*. The University of British Columbia.

Beamish, A. L., Nijland, W., Edwards, M., Coops, N. C., & Henry, G. H. R. (2016). Phenology and vegetation change measurements from true colour digital photography in high Arctic tundra. *Arctic Science*, *2*(2), 33–49. https://doi.org/10.1139/as-2014-0003

Betway-May, K. R., Hollister, R. D., May, J. L., Harris, J. A., Gould, W. A., & Oberbauer, S. F. (2022). Can plant functional traits explain shifts in community composition in a changing Arctic? *Arctic Science*, *8*(3), 899–915. https://doi.org/10.1139/as-2020-0036

Billings, W. D., Godfrey, P. J., Chabot, B. F., & Bourque, D. P. (1971). Metabolic Acclimation to Temperature in Arctic and Alpine Ecotypes of Oxyr1A Digyna. *Arctic and Alpine Research*, *3*(4), 277–289. https://doi.org/10.1080/00040851.1971.12003619

Bivand, R., Keitt, T., Rowlingson, B., Pebesma, E., Sumner, M., Hijmans, R., Baston, D., Rouault, E., Warmerdam, F., Ooms, J., & Rundel, C. (2023). *rgdal: Bindings for the "Geospatial" Data Abstraction Library* (1.6-5). https://CRAN.R-project.org/package=rgdal

Bjorkman, A. D., Elmendorf, S. C., Beamish, A. L., Vellend, M., & Henry, G. H. R. (2015). Contrasting effects of warming and increased snowfall on Arctic tundra plant phenology over the past two decades. *Global Change Biology*, *21*(12), 4651–4661. https://doi.org/10.1111/gcb.13051

Bjorkman, A. D., Myers-Smith, I. H., Elmendorf, S. C., Normand, S., Rüger, N., Beck, P. S. A., Blach-Overgaard, A., Blok, D., Cornelissen, J. H. C., Forbes, B. C., Georges, D., Goetz, S. J., Guay, K. C., Henry, G. H. R., HilleRisLambers, J., Hollister, R. D., Karger, D. N., Kattge, J., Manning, P., … Weiher, E. (2018). Plant functional trait change across a warming tundra biome. *Nature*, *562*(7725), Article 7725. https://doi.org/10.1038/s41586-018-0563-7

Boelman, N. T., Stieglitz, M., Rueth, H. M., Sommerkorn, M., Griffin, K. L., Shaver, G. R., & Gamon, J. A. (2003). Response of NDVI, biomass, and ecosystem gas exchange to

long-term warming and fertilization in wet sedge tundra. *Oecologia*, *135*(3), 414–421. https://doi.org/10.1007/s00442-003-1198-3

Cahoon, S. M. P., Sullivan, P. F., Shaver, G. R., Welker, J. M., & Post, E. (2012). Interactions among shrub cover and the soil microclimate may determine future Arctic carbon budgets. *Ecology Letters*, *15*(12), 1415–1422. https://doi.org/10.1111/j.1461-0248.2012.01865.x

Campioli, M., Schmidt, N. M., Albert, K. R., Leblans, N., Ro-poulsen, H., & Michelsen, A. (2013). Does warming affect growth rate and biomass production of shrubs in the High Arctic? *Plant Ecology*, *214*(8), 1049–1058. https://doi.org/10.1007/s11258-013-0230-x

Christiansen, C. T., Schmidt, N. M., & Michelsen, A. (2012). High Arctic Dry Heath CO2 Exchange During the Early Cold Season. *Ecosystems*, *15*(7), 1083–1092. https://doi.org/10.1007/s10021-012-9569-4

Constable, A. J., Harper, S., Dawson, J., Holsman, K., Mustonen, T., Piepenburg, D., & Rost, B. (2022). Cross-Chapter Paper 6: Polar Regions Supplementary Material. In H.-O. Pörtner, D. C. Roberts, M. Tignor, E. S. Poloczanska, K. Mintenbeck, A. Alegría, M. Craig, S. Langsdorf, S. Löschke, V. Möller, A. Okem, & B. Rama (Eds.), *Climate Change 2022: Impacts, Adaptation, and Vulnerability. Contribution of Working Group II to the Sixth Assessment Report of the Intergovernmental Panel on Climate Change*. https://www.ipcc.ch/report/ar6/wg2/

Davidson, E. A., & Janssens, I. A. (2006). Temperature sensitivity of soil carbon decomposition and feedbacks to climate change. *Nature*, *440*(7081), Article 7081. https://doi.org/10.1038/nature04514

Derksen, C., Burgess, D., Duguay, C., Howell, S., Mudryk, L., Smith, S., & al, et. (2019). Changes in Snow, Ice, and Permafrost Across Canada. In E. Bush & D. S. Lemmen (Eds.), *Canada's Changing Climate Report* (pp. 194–260). Government of Canada.

Edwards, M. (2012). *Effects of long-term experimental warming on three High Arctic plant communities* [M.S. Thesis, University of British Columbia]. https://doi.org/10.14288/1.0072736

Edwards, M., & Henry, G. H. R. (2016). The effects of long-term experimental warming on the structure of three High Arctic plant communities. *Journal of Vegetation Science*, *27*(5), 904–913. https://doi.org/10.1111/jvs.12417

Elmendorf, S. C., Henry, G. H. R., Hollister, R. D., Björk, R. G., Bjorkman, A. D., Callaghan, T. V., Collier, L. S., Cooper, E. J., Cornelissen, J. H. C., Day, T. A., Fosaa, A. M., Gould, W. A., Grétarsdóttir, J., Harte, J., Hermanutz, L., Hik, D. S., Hofgaard, A., Jarrad, F., Jónsdóttir, I. S., … Wookey, P. A. (2012). Global assessment of experimental climate warming on tundra vegetation: Heterogeneity over space and time. *Ecology Letters*, *15*(2), 164–175. https://doi.org/10.1111/j.1461-0248.2011.01716.x

Elmendorf, S. C., Henry, G. H. R., Hollister, R. D., Björk, R. G., Boulanger-Lapointe, N., Cooper, E. J., Cornelissen, J. H. C., Day, T. A., Dorrepaal, E., Elumeeva, T. G., Gill, M., Gould, W. A., Harte, J., Hik, D. S., Hofgaard, A., Johnson, D. R., Johnstone, J. F., Jónsdóttir, I. S., Jorgenson, J. C., … Wipf, S. (2012). Plot-scale evidence of tundra vegetation change and links to recent summer warming. *Nature Climate Change*, *2*(6), Article 6. https://doi.org/10.1038/nclimate1465

Evans, J. R. (1989). Photosynthesis and nitrogen relationships in leaves of C3 plants. *Oecologia*, *78*(1), 9–19. https://doi.org/10.1007/BF00377192

Finderup Nielsen, T., Ravn, N. R., & Michelsen, A. (2019). Increased CO2 efflux due to long-term experimental summer warming and litter input in subarctic tundra – CO2 fluxes at snowmelt, in growing season, fall and winter. *Plant and Soil*, *444*(1), 365–382. https://doi.org/10.1007/s11104-019-04282-9

Freedman, B., Svoboda, J., & Henry, G. H. R. (1994). Alexandra Fiord–An ecological oasis in the polar desert. In J. Svoboda & B. Freedman (Eds.), *Ecology of a polar oasis: Alexandra Fiord, Ellesmere Island, Canada* (pp. 1–9). Captus Univ. Publ.

Frei, E. R., & Henry, G. H. R. (2021). Long-term effects of snowmelt timing and climate warming on phenology, growth, and reproductive effort of Arctic tundra plant species. *Arctic Science*, 1–22. https://doi.org/10.1139/as-2021-0028

Grant, R. F., Humphreys, E. R., Lafleur, P. M., & Dimitrov, D. D. (2011). Ecological controls on net ecosystem productivity of a mesic arctic tundra under current and future climates. *Journal of Geophysical Research. Biogeosciences*, *116*(1). https://doi.org/10.1029/2010JG001555

Grolemund, G., & Wickham, H. (2011). Dates and Times Made Easy with lubridate. *Journal of Statistical Software*, *40*(3), 1–25.

Happonen, K., Virkkala, A.-M., Kemppinen, J., Niittynen, P., & Luoto, M. (2022). Relationships between above-ground plant traits and carbon cycling in tundra plant communities. *Journal of Ecology*, *110*(3), 700–716. https://doi.org/10.1111/1365-2745.13832

Henry, G. H. R., Hollister, R. D., Klanderud, K., Björk, R. G., Bjorkman, A. D., Elphinstone, C., Jónsdóttir, I. S., Molau, U., Petraglia, A., Oberbauer, S. F., Rixen, C., & Wookey, P. A. (2022). The International Tundra Experiment (ITEX): 30 years of research on tundra ecosystems. *Arctic Science*, *8*(3), 550–571. https://doi.org/10.1139/as-2022-0041

Hobbie, S. E., & Chapin, F. S. (1998). The response of tundra plant biomass, aboveground production, nitrogen, and co2 flux to experimental warming. *Ecology*, *79*(5), 1526–1544.

Hollister, R. D., Elphinstone, C., Henry, G. H. R., Bjorkman, A. D., Klanderud, K., Björk, R. G., Björkman, M. P., Bokhorst, S., Carbognani, M., Cooper, E. J., Dorrepaal, E., Elmendorf, S. C., Fetcher, N., Gallois, E. C., Guðmundsson, J., Healey, N. C., Jónsdóttir, I. S., Klarenberg, I. J., Oberbauer, S. F., … Wookey, P. A. (2022). A review of open top chamber (OTC) performance across the ITEX Network. *Arctic Science*. https://doi.org/10.1139/as-2022-0030

Hudson, J. M. G., & Henry, G. H. R. (2009). Increased plant biomass in a High Arctic heath community from 1981 to 2008. *Ecology*, *90*(10), 2657–2663. https://doi.org/10.1890/09-0102.1

Hudson, J. M. G., Henry, G. H. R., & Cornwell, W. K. (2011). Taller and larger: Shifts in Arctic tundra leaf traits after 16 years of experimental warming. *Global Change Biology*, *17*(2), 1013–1021. https://doi.org/10.1111/j.1365-2486.2010.02294.x

Huemmrich, K. F., Kinoshita, G., Gamon, J. A., Houston, S., Kwon, H., & Oechel, W. C. (2010). Tundra carbon balance under varying temperature and moisture regimes. *Journal of Geophysical Research: Biogeosciences*, *115*(G4). https://doi.org/10.1029/2009JG001237

Hugelius, G., Strauss, J., Zubrzycki, S., Harden, J. W., Schuur, E. a. G., Ping, C.-L., Schirrmeister, L., Grosse, G., Michaelson, G. J., Koven, C. D., O'Donnell, J. A., Elberling, B., Mishra, U., Camill, P., Yu, Z., Palmtag, J., & Kuhry, P. (2014). Estimated stocks of circumpolar permafrost carbon with quantified uncertainty ranges and

identified data gaps. *Biogeosciences*, *11*(23), 6573–6593. https://doi.org/10.5194/bg-11-6573-2014

Jónsdóttir, I. S., Halbritter, A. H., Christiansen, C. T., Althuizen, I. H. J., Haugum, S. V., Henn, J. J., Björnsdóttir, K., Maitner, B. S., Malhi, Y., Michaletz, S. T., Roos, R. E., Klanderud, K., Lee, H., Enquist, B. J., & Vandvik, V. (2022). Intraspecific trait variability is a key feature underlying high Arctic plant community resistance to climate warming. *Ecological Monographs*, *93*(1), e1555. https://doi.org/10.1002/ecm.1555

Knoblauch, C., Beer, C., Sosnin, A., Wagner, D., & Pfeiffer, E.-M. (2013). Predicting long-term carbon mineralization and trace gas production from thawing permafrost of Northeast Siberia. *Global Change Biology*, *19*(4), 1160–1172. https://doi.org/10.1111/gcb.12116

Koven, C. D., Ringeval, B., Friedlingstein, P., Ciais, P., Cadule, P., Khvorostyanov, D., Krinner, G., & Tarnocai, C. (2011). Permafrost carbon-climate feedbacks accelerate global warming. *Proceedings of the National Academy of Sciences*, *108*(36), 14769–14774. https://doi.org/10.1073/pnas.1103910108

Kutzbach, L., Schneider, J., Sachs, T., Giebels, M., Nykanen, H., Shurpali, N. J., Martikainen, P. J., Alm, J., & Wilmking, M. (2007). *CO2 flux determination by closed-chamber methods can be seriously biased by inappropriate application of linear regression*. 21.

Kuznetsova, A., Brockhoff, P. B., & Christensen, R. H. B. (2017). lmerTest Package: Tests in Linear Mixed Effects Models. *Journal of Statistical Software*, *82*(13), 1–26. https://doi.org/10.18637/jss.v082.i13

Kwon, H.-J., Oechel, W. C., Zulueta, R. C., & Hastings, S. J. (2006). Effects of climate variability on carbon sequestration among adjacent wet sedge tundra and moist

tussock tundra ecosystems. *Journal of Geophysical Research: Biogeosciences*, *111*(G3). https://doi.org/10.1029/2005JG000036

Kwon, M. J., Natali, S. M., Hicks Pries, C. E., Schuur, E. A. G., Steinhof, A., Crummer, K. G., Zimov, N., Zimov, S. A., Heimann, M., Kolle, O., & Göckede, M. (2019). Drainage enhances modern soil carbon contribution but reduces old soil carbon contribution to ecosystem respiration in tundra ecosystems. *Global Change Biology*, *25*(4), 1315–1325. https://doi.org/10.1111/gcb.14578

Lafleur, P. M., Humphreys, E. R., St. Louis, V. L., Myklebust, M. C., Papakyriakou, T., Poissant, L., Barker, J. D., Pilote, M., & Swystun, K. A. (2012). Variation in Peak Growing Season Net Ecosystem Production Across the Canadian Arctic. *Environmental Science & Technology*, *46*(15), 7971–7977. https://doi.org/10.1021/es300500m

Liu, X., Dong, W., Wood, J. D., Wang, Y., Li, X., Zhang, Y., Hu, C., & Gu, L. (2022). Aboveground and belowground contributions to ecosystem respiration in a temperate deciduous forest. *Agricultural and Forest Meteorology*, *314*, 108807. https://doi.org/10.1016/j.agrformet.2022.108807

Lüdecke, D., Ben-Shachar, M. S., Patil, I., Waggoner, P., & Makowski, D. (2021). performance: An R Package for Assessment, Comparison and Testing of Statistical Models. *Journal of Open Source Software*, *6*(60), 3139. https://doi.org/10.21105/joss.03139

Lupascu, M., Welker, J. M., Seibt, U., Maseyk, K., Xu, X., & Czimczik, C. I. (2014). High Arctic wetting reduces permafrost carbon feedbacks to climate warming. *Nature Climate Change*, *4*(1), Article 1. https://doi.org/10.1038/nclimate2058

Marchand, F. L., Nijs, I., de Boeck, H. J., Kockelbergh, F., Mertens, S., & Beyens, L. (2004). Increased Turnover but Little Change in the Carbon Balance of High-Arctic Tundra

Exposed to Whole Growing Season Warming. *Arctic, Antarctic, and Alpine Research*, *36*(3), 298–307. https://doi.org/10.1657/1523-0430(2004)036[0298:ITBLCI]2.0.CO;2

Marion, G. m., Henry, G. h. r., Freckman, D. w., Johnstone, J., Jones, G., Jones, M. h., Lévesque, E., Molau, U., Mølgaard, P., Parsons, A. n., Svoboda, J., & Virginia, R. a. (1997). Open-top designs for manipulating field temperature in high-latitude ecosystems. *Global Change Biology*, *3*(S1), 20–32. https://doi.org/10.1111/j.1365-2486.1997.gcb136.x

McFadden, J. P., Eugster, W., & Chapin, F. S. (2003). A Regional Study of the Controls on Water Vapor and CO2 Exchange in Arctic Tundra. *Ecology*, *84*(10), 2762–2776.

McGuire, A. D., Anderson, L. G., Christensen, T. R., Dallimore, S., Guo, L., Hayes, D. J., Heimann, M., Lorenson, T. D., Macdonald, R. W., & Roulet, N. (2009). Sensitivity of the carbon cycle in the Arctic to climate change. *Ecological Monographs*, *79*(4), 523–555. https://doi.org/10.1890/08-2025.1

Mekonnen, Z. A., Riley, W. J., Berner, L. T., Bouskill, N. J., Torn, M. S., Iwahana, G., Breen, A. L., Myers-Smith, I. H., Criado, M. G., Liu, Y., Euskirchen, E. S., Goetz, S. J., Mack, M. C., & Grant, R. F. (2021). Arctic tundra shrubification: A review of mechanisms and impacts on ecosystem carbon balance. *Environmental Research Letters*, *16*(5), 053001. https://doi.org/10.1088/1748-9326/abf28b

Mekonnen, Z. A., Riley, W. J., & Grant, R. F. (2018). 21st century tundra shrubification could enhance net carbon uptake of North America Arctic tundra under an RCP8.5 climate trajectory. *Environmental Research Letters*, *13*(5), 054029. https://doi.org/10.1088/1748-9326/aabf28

Nijland, W., de Jong, R., de Jong, S. M., Wulder, M. A., Bater, C. W., & Coops, N. C. (2014). Monitoring plant condition and phenology using infrared sensitive consumer grade

digital cameras. *Agricultural and Forest Meteorology*, *184*, 98–106. https://doi.org/10.1016/j.agrformet.2013.09.007

Oberbauer, S. F., Tweedie, C. E., Welker, J. M., Fahnestock, J. T., Henry, G. H. R., Webber, P. J., Hollister, R. D., Walker, M. D., Kuchy, A., Elmore, E., & Starr, G. (2007). Tundra CO2 Fluxes in Response to Experimental Warming across Latitudinal and Moisture Gradients. *Ecological Monographs*, *77*(2), 221–238.

Pirk, N., Tamstorf, M. P., Lund, M., Mastepanov, M., Pedersen, S. H., Mylius, M. R., Parmentier, F.-J. W., Christiansen, H. H., & Christensen, T. R. (2016). Snowpack fluxes of methane and carbon dioxide from high Arctic tundra. *Journal of Geophysical Research: Biogeosciences*, *121*(11), 2886–2900. https://doi.org/10.1002/2016JG003486

Powers, S. M., & Hampton, S. E. (2019). Open science, reproducibility, and transparency in ecology. *Ecological Applications*, *29*(1), e01822. https://doi.org/10.1002/eap.1822

R Core Team. (2022). *R: A Language and Environment for Statistical Computing*. R Foundation for Statistical Computing. https://www.R-project.org/

Rantanen, M., Karpechko, A. Y., Lipponen, A., Nordling, K., Hyvärinen, O., Ruosteenoja, K., Vihma, T., & Laaksonen, A. (2022). The Arctic has warmed nearly four times faster than the globe since 1979. *Communications Earth & Environment*, *3*(1), Article 1. https://doi.org/10.1038/s43247-022-00498-3

Sandve, G. K., Nekrutenko, A., Taylor, J., & Hovig, E. (2013). Ten Simple Rules for Reproducible Computational Research. *PLOS Computational Biology*, *9*(10), e1003285. https://doi.org/10.1371/journal.pcbi.1003285

Schuur, E. a. G., McGuire, A. D., Schädel, C., Grosse, G., Harden, J. W., Hayes, D. J., Hugelius, G., Koven, C. D., Kuhry, P., Lawrence, D. M., Natali, S. M., Olefeldt, D., Romanovsky,

V. E., Schaefer, K., Turetsky, M. R., Treat, C. C., & Vonk, J. E. (2015). Climate change and the permafrost carbon feedback. *Nature*, *520*(7546), Article 7546. https://doi.org/10.1038/nature14338

Segal, A. D. (2013). *Root and microbial respiration dominate carbon dioxide efflux in an arctic ecosystem* [M.S. Thesis, University of Alaska Anchorage]. https://www.proquest.com/docview/1314999512/abstract/3D5428355B6E41D8PQ/1

Shaver, G. R., Canadell, J., Chapin, F. S., Gurevitch, J., & al, et. (2000). Global warming and terrestrial ecosystems: A conceptual framework for analysis. *Bioscience*, *50*(10), 871–882. https://doi.org/10.1641/0006-3568(2000)050[0871:GWATEA]2.0.CO;2

Shaver, G. R., Johnson, L. C., Cades, D. H., Murray, G., Laundre, J. A., Rastetter, E. B., Nadelhoffer, K. J., & Giblin, A. E. (1998). Biomass and CO2 flux in wet sedge tundras: Responses to nutrients, temperature, and light. *Ecological Monographs*, *68*(1), 75–97. https://doi.org/10.1890/0012-9615(1998)068[0075:BACFIW]2.0.CO;2

Skeeter, J., Christen, A., & Henry, G. H. R. (2022). Controls on carbon dioxide and methane fluxes from a low-center polygonal peatland in the Mackenzie River Delta, Northwest Territories. *Arctic Science*, *8*(2), 471–497. https://doi.org/10.1139/as-2021-0034

Skeeter, J., Christen, A., Laforce, A.-A., Humphreys, E., & Henry, G. (2020). Vegetation influence and environmental controls on greenhouse gas fluxes from a drained thermokarst lake in the western Canadian Arctic. *Biogeosciences*, *17*(17), 4421–4441. https://doi.org/10.5194/bg-17-4421-2020

Street, L. E., Shaver, G. R., Williams, M., & Van Wijk, M. T. (2007). What is the relationship between changes in canopy leaf area and changes in photosynthetic CO2 flux in

arctic ecosystems? *Journal of Ecology*, *95*(1), 139–150. https://doi.org/10.1111/j.1365-2745.2006.01187.x

Tarnocai, C., Canadell, J. G., Schuur, E. a. G., Kuhry, P., Mazhitova, G., & Zimov, S. (2009). Soil organic carbon pools in the northern circumpolar permafrost region. *Global Biogeochemical Cycles*, *23*(2). https://doi.org/10.1029/2008GB003327

Tieszen, L. L. (1973). Photosynthesis and Respiration in Arctic Tundra Grasses: Field Light Intensity and Temperature Responses. *Arctic and Alpine Research*, *5*(3), 239–251. https://doi.org/10.2307/1550031

Uchida, M., Muraoka, H., & Nakatsubo, T. (2016). Sensitivity analysis of ecosystem CO2 exchange to climate change in High Arctic tundra using an ecological process-based model. *Polar Biology*, *39*(2), 251–265. https://doi.org/10.1007/s00300-015-1777-x

Virkkala, A.-M., Virtanen, T., Lehtonen, A., Rinne, J., & Luoto, M. (2018). The current state of CO2 flux chamber studies in the Arctic tundra: A review. *Progress in Physical Geography: Earth and Environment*, *42*(2), 162–184. https://doi.org/10.1177/0309133317745784

Welker, J. M., Fahnestock, J. T., Henry, G. H. R., O'Dea, K. W., & Chimner, R. A. (2004). CO2 exchange in three Canadian High Arctic ecosystems: Response to long-term experimental warming. *Global Change Biology*, *10*(12), 1981–1995. https://doi.org/10.1111/j.1365-2486.2004.00857.x

Wickham, H., Averick, M., Bryan, J., Chang, W., McGowan, L. D., François, R., Grolemund, G., Hayes, A., Henry, L., Hester, J., Kuhn, M., Pedersen, T. L., Miller, E., Bache, S. M., Müller, K., Ooms, J., Robinson, D., Seidel, D. P., Spinu, V., … Yutani, H. (2019). Welcome to the tidyverse. *Journal of Open Source Software*, *4*(43), 1686. https://doi.org/10.21105/joss.01686

Supplementary Materials

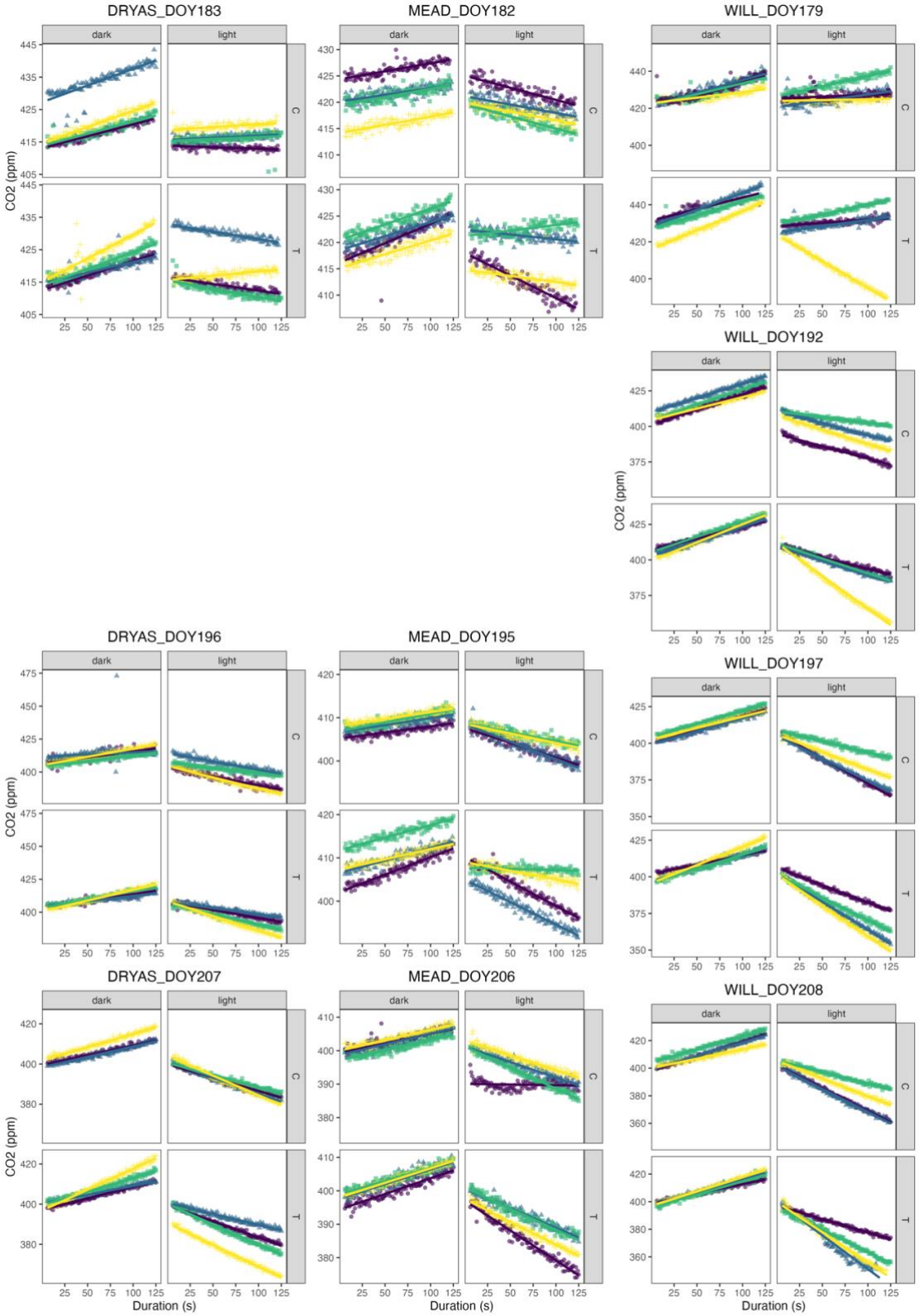

Figure S1. Raw flux data from the infrared gas analyzer separated by site, collection day (DOY), treatment (C/T), and flux, where dark is the ER measurement and light is the NEE measurement. Trendlines are basic linear models fit to each flux by plot.

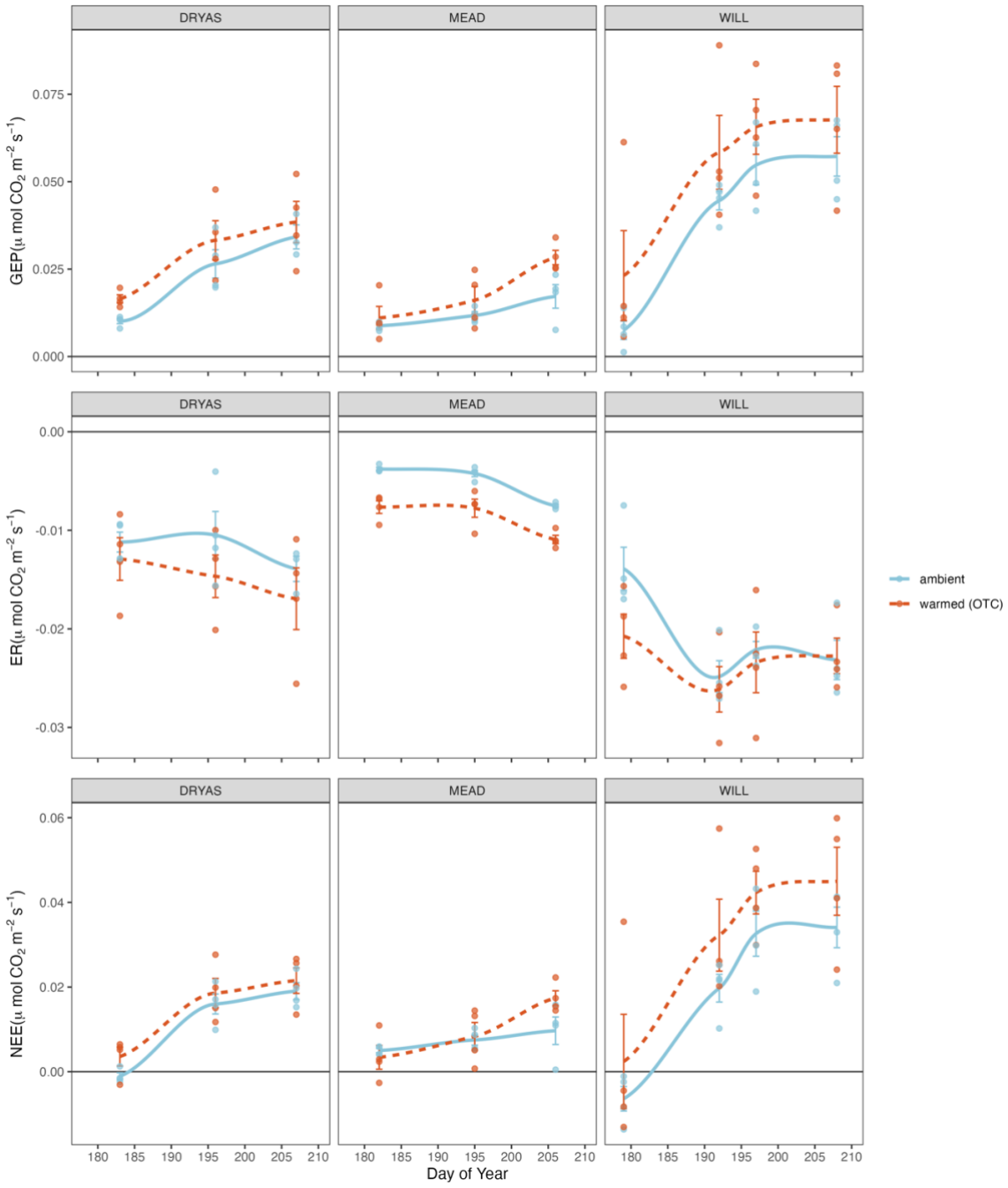

Figure S2. Carbon fluxes in µmol CO_2 m-2 s-1 over time. Error bars display the standard error about the mean flux value at each observation time. Each point represents a linear model fit to CO_2 concentration measurements over a two-minute interval.

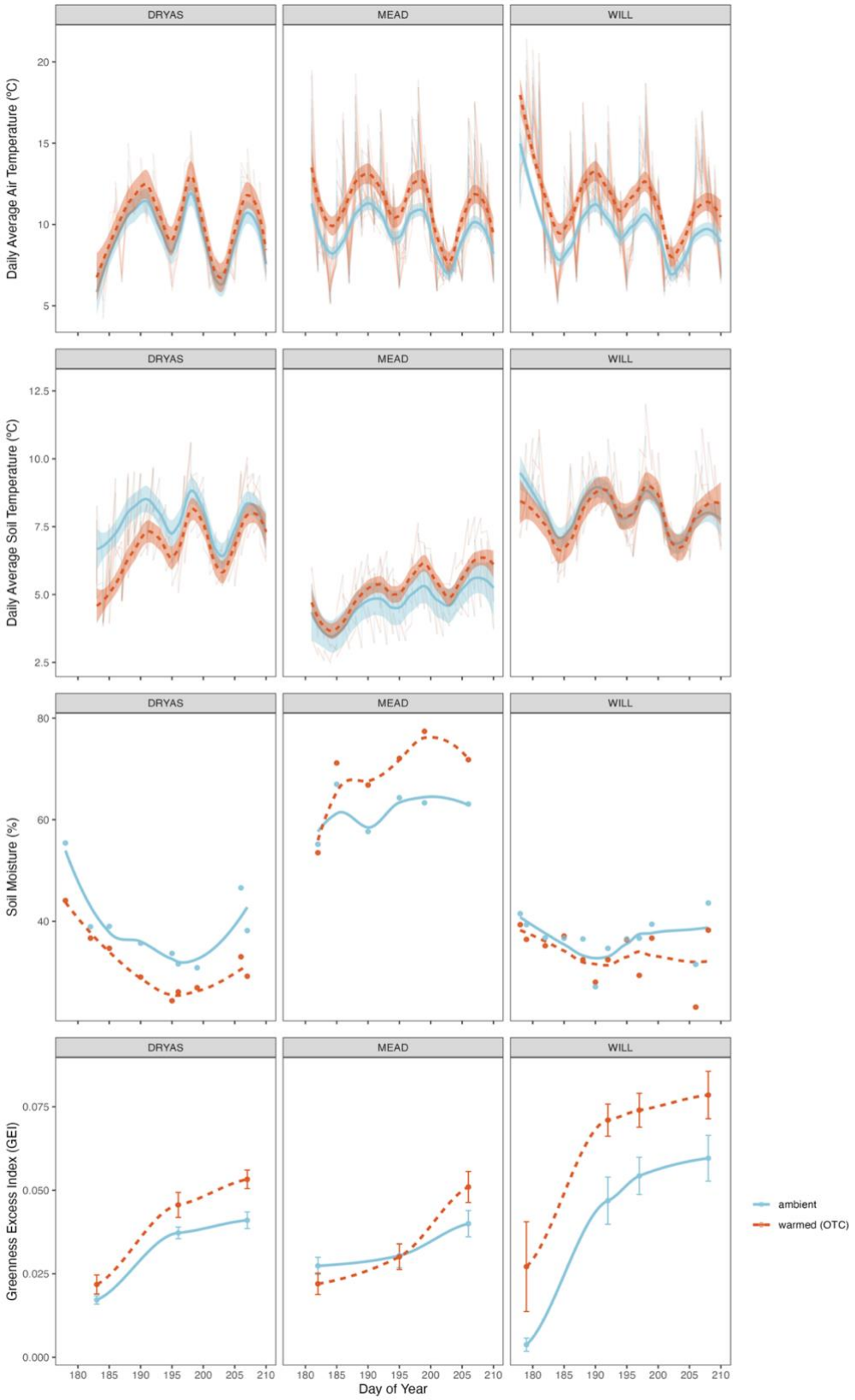

Figure S3. Mean daily air and soil temperature, soil moisture, and greenness excess index (GEI) over the growing season. Trendlines represent smoothed conditional means to help illustrate temporal trends in the data.

Supplementary Table 1. Linear mixed effects model output from lmerTest with NEE as the response variable, treatment as a fixed effect and site, plot as random effects.

NEE ~ treatment + (1|site/plot) | Conditional R^2 = 0.272, Marginal R2 = 0.030						
	Estimate	Std. Error	df	t value	Pr(>|t|)	
(Intercept)	0.012746	0.005297	2.478039	2.406	0.1134	
treatmentT	0.005857	0.003257	69.194974	1.798	0.0765	.

Supplementary Table 2. Linear mixed effects model output from lmerTest with ER as the response variable, treatment as a fixed effect and site, plot as random effects.

ER ~ treatment + (1|site/plot) | Conditional R^2: 0.807, Marginal R^2: 0.029						
	Estimate	Std. Error	df	t value	Pr(>|t|)	
(Intercept)	-0.0126643	0.0044194	2.0427501	-2.866	0.10079	
treatmentT	-0.0029292	0.0008615	65.6603791	-3.4	0.00115	**

Supplementary Table 3. Linear mixed effects model output from lmerTest with ER as the response variable, treatment as a fixed effect and site, plot as random effects.

GEP ~ treatment + (1|site/plot) | Conditional R^2: 0.482, Marginal R^2: 0.035						
	Estimate	Std. Error	df	t value	Pr(>|t|)	
(Intercept)	0.02524	0.009612	2.194073	2.626	0.1087	
treatmentT	0.008918	0.003875	68.067573	2.301	0.0245	*

Supplementary Table 4. Least squares means table with NEE as the response variable, treatment and site as fixed effects, and plot as a random effect.

NEE ~ treatment + site + (1|site:plot) | Conditional R^2: 0.237, Marginal R^2: 0.226								
	Estimate	Std. Error	df	t value	lower	upper	Pr(>|t|)	
treatmentC - treatmentT	-0.00586	0.00326	69.2	-1.7979	-0.01236	0.00064	0.07655	.
siteDRYAS - siteMEAD	0.00439	0.00438	14.0	1.0019	-0.00501	0.01379	0.33336	
siteDRYAS - siteWILL	-0.01231	0.00412	11.1	-2.9855	-0.02137	-0.00325	0.01225	*
siteMEAD - siteWILL	-0.01670	0.00412	11.1	-4.0506	-0.02576	-0.00764	0.00187	**

Supplementary Table 5. Least squares means table with GEP as the response variable, treatment and site as fixed effects, and plot as a random effect.

GEP ~ treatment + site + (1|site:plot) | Conditional R^2: 0.417, Marginal R^2: 0.414								
	Estimate	Std. Error	df	t value	lower	upper	Pr(>|t|)	
treatmentC - treatmentT	-0.00892	0.00388	68.1	-2.3022	-0.01666	-0.00119	0.02439	*
siteDRYAS - siteMEAD	0.01044	0.00511	13.8	2.0424	-0.00053	0.02142	0.06063	.
siteDRYAS - siteWILL	-0.02141	0.00480	10.9	-4.4585	-0.03199	-0.01083	0.00099	***
siteMEAD - siteWILL	-0.03185	0.00474	10.4	-6.7135	-0.04236	-0.02134	0.00004	***

Supplementary Table 6. Least squares means table with ER as the response variable, treatment and site as fixed effects, and plot as a random effect.

ER ~ treatment + site + (1|site:plot), Conditional R^2: 0.758, Marginal R^2: 0.721								
	Estimate	Std. Error	df	t value	lower	upper	Pr(>|t|)	
treatmentC - treatmentT	0.00293	0.00086	65.7	3.40060	0.00121	0.00465	0.00115	**
siteDRYAS - siteMEAD	-0.00628	0.00154	9.5	-4.07750	-0.00973	-0.00282	0.00248	**
siteDRYAS - siteWILL	0.00887	0.00149	8.3	5.95800	0.00546	0.01228	0.00029	***
siteMEAD - siteWILL	0.01515	0.00148	8.1	10.23980	0.01174	0.01855	0.00001	***

Supplementary Table 7. Backwards selected NEE model output from lmerTest with treatment, site, GEI, soil moisture, and air temperature as fixed effects and plot as a random effect.

Backward reduced fixed-effect table: NEE ~ GEI + (1 | site:plot), Conditional R^2: 0.863, Marginal R^2: 0.822								
Degrees of freedom method: Satterthwaite								
	Eliminated	Sum Sq	Mean Sq	NumDF	DenDF	F value	Pr(>F)	
T_air	1	0.0000019	0.0000019	1	68.885	0.0548	0.8155	
soil_moisture	2	0.0000067	0.0000067	1	71.458	0.1946	0.6605	
site	3	0.0000816	0.0000408	2	10.201	1.1979	0.341	
treatment	4	0.0000855	0.0000855	1	67.171	2.504	0.1183	
GEI	0	0.0143724	0.0143724	1	74.95	414.2193	<2e-16	***
Backward reduced random-effect table:								
	Eliminated	npar	logLik	AIC	LRT	Df	Pr(>Chisq)	
<none>		9	254.08	-490.17				
(1 | site:plot)	0	8	250.93	-485.85	6.3187	1	0.01195	*
Final model parameters								
	Estimate	Std. Error	df	t value	Pr (>|t|)			
(Intercept)	-0.011531	0.001767	43.988409	-6.525	5.71E-08		***	
GEI	0.67168	0.033003	74.949675	20.352	< 2.00E-16		***	

Supplementary Table 8. Backwards selected ER model output from lmerTest with treatment, site, GEI, soil moisture, and air temperature as fixed effects and plot as a random effect.

Backward reduced fixed-effect table: ER ~ treatment + site + GEI + (1 | site:plot), Conditional R^2: 0.846, Marginal R^2: 0.797								
Degrees of freedom method: Satterthwaite								
	Eliminated	Sum Sq	Mean Sq	NumDF	DenDF	F value	Pr(>F)	
soil_moisture	1	0.00000126	0.00000126	1	68.5	0.1335	0.716	
T_air	2	0.00000603	0.00000603	1	66.643	0.6519	0.4223	
treatment	0	0.00004284	0.00004284	1	64.997	4.6477	0.0348	*
site	0	0.00068155	0.00034077	2	9.329	36.9684	3.68E-05	***

GEI	0	0.00036758	0.00036758	1	66.289	39.8763	2.59E-08	***
Backward reduced random-effect table:								
	Eliminated	npar	logLik	AIC	LRT	Df	Pr(>Chisq)	
<none>		9	297.4	-576.79				
(1 | site:plot)	0	8	294.6	-573.2	5.5891	1	0.01807	*
Final model parameters								
	Estimate	Std. Error	df	t value	Pr (>|t|)			
(Intercept)	-0.008343	0.001258	17.276325	-6.633	3.90E-06	***		
treatmentT	-0.001548	0.000718	64.997247	-2.156	0.0348	*		
siteMEAD	0.006026	0.001515	9.358372	3.978	0.00298	**		
siteWILL	-0.006983	0.001512	9.286156	-4.618	0.00116	**		

Supplementary Table 9. Backwards selected GEP model output from lmerTest with treatment, site, GEI, soil moisture, and air temperature as fixed effects and plot as a random effect.

Backward reduced fixed-effect table: GEP ~ treatment + site + GEI + (1 | site:plot), Conditional R^2: 0.848, Marginal R^2: 0.799							
Degrees of freedom method: Satterthwaite							
	Eliminated	Sum Sq	Mean Sq	NumDF	DenDF	F value	Pr(>F)
T_air	1	0.0000010	0.0000010	1	67.497	0.0208	0.885821
treatment	2	0.0000028	0.0000028	1	64.523	0.0589	0.809033
soil_moisture	3	0.0000184	0.0000184	1	71.054	0.3874	0.535642
site	0	0.0012292	0.0006146	2	9.725	13.1029	1.74E-03 **
GEI	0	0.0186637	0.0186637	1	67.566	397.9046	< 2.2e-16 ***
Backward reduced random-effect table:							
	Eliminated	npar	logLik	AIC	LRT	Df	Pr(>Chisq)
<none>		9	238.18	-458.36			
(1 | site:plot)	0	8	235.02	-454.04	6.3214	1	0.01193 *
Final model parameters							
	Estimate	Std. Error	df	t value	Pr (>|t|)		
(Intercept)	-0.002151	0.002796	17.484044	-0.769	0.452		
siteMEAD	-0.008711	0.003395	9.81802	-2.566	0.0285	*	
siteWILL	0.008623	0.003381	9.647215	2.551	0.0296	*	
GEI	0.788429	0.039525	67.565897	19.948	<2e-16	***	